Article

Effect of HVAC's Management on Indoor Thermo-Hygrometric Comfort and Energy Balance: In Situ Assessments on a Real nZEB

Rosa Francesca De Masi [1,*]**, Antonio Gigante** [1]**, Valentino Festa** [1]**, Silvia Ruggiero** [1] **and Giuseppe Peter Vanoli** [2]

[1]   DING—Department of Engineering, University of Sannio, 82100 Benevento, Italy;
    gigante@unisannio.it (A.G.); valefesta@unisannio.it (V.F.); sruggiero@unisannio.it (S.R.)
[2]   Department of Medicine and Health Sciences—Vincenzo Tiberio, University of Molise,
    86100 Campobasso, Italy; giuseppe.vanoli@unimol.it
*   Correspondence: rfdemasi@unisannio.it; Tel.: +39-0824-305577

Abstract: This paper proposes the analysis of real monitored data for evaluating the relationship between occupants' comfort conditions and the energy balance inside an existing, nearly zero-energy building under different operational strategies for the heating, ventilation, and air-conditioning system. During the wintertime, the adaptive comfort approach is applied for choosing the temperature setpoint when an air-to-air heat pump provides both heating and ventilation. The results indicate that in very insulated buildings with high solar gains, the setpoint should be decided taking into consideration both the solar radiation and the outdoor temperature. Indeed, when the room has large glazed surfaces, the solar radiation can also guarantee acceptable indoor conditions when a low setpoint (e.g., 18.7 °C) is considered. The electricity consumption can be reduced from 17% to 43% compared to a conventional setpoint (e.g., 20 °C). For the summertime, the analysis suggests the adoption of a dynamic approach that should be based on the outdoor conditions and differentiated according to room characteristics. Considering the indoor comfort and the maximization of renewable integration, the direct expansion system has better performance than the heat pump; this last system should be integrated with a pre-handling unit to be energy convenient.

Keywords: nZEB; HVAC management; monitoring campaign; indoor comfort; load matching; computational fluid dynamics

1. Introduction

A key element in order to achieve energy-efficient buildings with high integration of renewable sources is the adopted strategy of nearly zero-energy buildings (nZEBs). According to the European Directive 2010/31 [1], starting from 31 December 2020, all new buildings must be nZEB, and the goal of a zero energy balance is also promoted [2] for the refurbishment of existing stock. The design of high-performance buildings requires us to fully understand the connection between indoor comfort and energy use [3], because the low energy demand should not compromise the occupants' wellness. At the same time, the analysis of operational behavior is important for understanding the connection between indoor comfort and energy use, as well as between on-site generation and the building's self-consumption. Therefore, as was underlined by Butera [4], the comfort conditions and the real-time energy balance are two key research fields.

With regard to the first aspect, some numerical analyses indicated that energy use could be reduced by choosing appropriate setpoints [5,6]; conversely, the adoption of only one thermostat may be deficient in certain occupancy cases [7,8]. Controller tuning by setpoint regulation often provides relatively low- or no-extra-cost solutions for existing buildings [9]. With the aim of reducing energy demand and mitigating energy poverty, adaptive thermal comfort should be considered rather than fixed or tightly specified parameters [10].

Most scheduling methods lack a systematic approach to ensuring consumption reduction and occupant comfort [11]. As shown by Guillén et al. [12], the heating energy saving that can be achieved by moving the set temperature from 20 °C to 19 °C is between 30% and 46% for a nZEB and between 13% and 23% for a traditional dwelling. Reda et al. [13] have found that the adoption of information and communication technologies for setting heating setback and indoor setpoint temperatures and for controlling mechanical ventilation can ensure consistent reductions of energy demand.

Thermal comfort is always affected by the energy efficiency of buildings and vice versa [14], but it is also indisputable that the adoption of extended comfort ranges can cause significant energy saving [15,16]. For an office building, Sánchez-García et al. [17] have found that daily setpoint temperatures based on the adaptive thermal comfort approach can cause a 74.6% reduction in energy demand and a 59.7% drop in energy consumption. For different climatic conditions, Ming et al. [18] have shown how the use of a dynamic comfort range can reduce the cooling demand by around 34% compared with a static temperature setpoint. Similarly, Mui et al. [19] have found that demand-controlled ventilation and an adaptive comfort temperature setpoint have energy-saving potential between 21.4% and 24.3% in a subtropical climate zone. With surveys in mechanically ventilated offices, Roussac et al. [20] have found a reduction of daily heating, ventilation, and air-conditioning energy use of about 6% when a static control strategy is applied; on the other hand, a dynamic control approach causes an energy saving of around 6.3%. Data analytics applied to an office building have found that an alternative HVAC (Heating, Ventilation, and Air-Conditioning system) schedule that can reduce energy consumption by, on average, 2.7% [21]. A new controller based on occupancy prediction makes energy savings up to 75% possible [22]. Traylor et al. [23], by means of EnergyPlus simulations, have found that savings up to 5–15% could be achieved by modulating indoor temperatures in cooling applications. The results of Kim et al. [24] have demonstrated that with a controller based on the temperature and humidity, the use of the HVAC system can be reduced due to the human capability to thermally adapt after reaching the comfort range of temperature. Jazizadehet et al. [25] have shown the potentials of integration of diffuser-level adaptive actuation with improvements in thermal comfort satisfaction and energy savings of around 25%. Recently, the role of the key enabling technologies has been experimentally verified by Lourenço et al. [26]. Moreover, Kalaimani et al. [27] have shown how energy use could be reduced during periods of low occupancy by choosing appropriate thermal setpoints.

Briefly, the interest in adaptive models has led to the definition of different theories for the management of the heating and cooling system based on the relation of the operative indoor temperature [28] with the mean outdoor temperature, also considering an extended monitoring of buildings with high performance [29]. However, these studies are mainly focused on tertiary buildings during the cooling period. Although wider acceptable temperature ranges have been included in international standards, adoption of the adaptive principles into design practice is still limited, mainly with reference to the winter period [30] and for residential high-efficiency buildings. Some in situ analyses [31] have shown that the performance of natural night ventilation depends highly on the external weather conditions, and especially on the outdoor temperature. However, some monitored data indicate that active and passive ventilation and shading systems, if manually controlled, cannot guarantee a high-quality indoor environment [32].

Findings from O'Donovan et al. [33] show that passive control strategies maintained comfortable internal conditions between 57% and 95% of the occupied hours, without the need for mechanical cooling. However, variable setpoints could favor a match between the load and productivity curves [34] with minimal loss in comfort [35].

Perhaps the gaps in the current literature suggest that one of the most important omissions in the current literature is the limited availability of real applications that testify the implications and improvements of an adaptive and dynamic control of the heating, cooling, and ventilation system in a nearly zero-energy building, as well as the evaluation of occupant's perceptions. Indeed, with reference to this aspect, there are no studies based

on in situ monitoring campaigns that evaluate the influence of a comfort control strategy on the building energy balance and the effect on local renewable sources adoption, or in other words, on the matching between energy demand and renewable production. More generally, there is a lack of data regarding the operational behavior and the energy performance of nZEBs in a real context. The available scientific literature is mainly focused on design strategies and not on the post-occupancy performance evaluation of this type of building. Instead, the occupants' behavior is widely recognized as a major factor in the disparity between predicted and measured building performance [36]. Therefore, hourly and sub-hourly analysis can give more accurate information compared with measured peak values [37]. The comparative analysis of O'Donovan et al. [38] has highlighted the need to consider diverse occupancy schedules and opening control strategies for evaluating the performance of nearly zero-energy buildings. In another study [39], the same authors have found that grey box modelling with an automatic model-calibration technique can reduce the human labor input for simulating the internal air temperature of a naturally ventilated nZEB by approximately 90%.

Considering that the integration of renewable energy sources is the key factor for achieving zero-energy performance, the second important issue is the evaluation of the impact of the uncertainty of renewable sources also in consideration of occupants' behavior. Indeed, the large-scale diffusion of nZEBs can affect the stability of the existing power grid with consequences on operational costs and environmental impacts. Real-time energy monitoring devices are significant tools for improving the load-matching between production and consumption [40]. Tumminia et al. [41], through some indicators, have underlined how the designing of a photovoltaic system able to cover the yearly estimated energy use has negative implications on the power grid. Aelenei et al. [42] have investigated the potential of increasing the load-matching by means of battery energy systems for improving the grid interaction. Demand-side management could bring various benefits such as: reduction in electricity cost, reduction in peak demand, and improvement in load factor [43]. Monitoring data from a real case study investigated by Stasi et al. [44] indicated that the energy performance gap concerning energy production on a yearly basis is equal to 9.1%, while on a monthly basis, the performance gap ranges from 3.5% to 27.1%. Demand-side management is one possible approach for reducing the electricity cost and peak demand, and for improving the load factor [43,45]. Moreover, because of extensive variations in occupancy patterns and their use of electrical equipment, accurate occupants' behavior detection is valuable for reducing a building's energy demand and carbon emissions [46].

This paper analyzes the interaction between these two aspects, and it proposes a critical post-occupancy analysis of a building designed to be nearly zero-energy, considering both the aspects connected to indoor thermal-hygrometric comfort and to the hourly energy balance between consumption and renewable production. With this aim, the results of a monitoring campaign and some numerical analysis are discussed, considering different HVAC settings. This kind of discussion is not available for other existing studies because research and national or international legislation are usually focused on long-term energy balances (based on annual or monthly time step), without considering that the energy exchange at a short time scale is often more critical. This case study is a single-story dwelling built in Benevento (South Italy, Mediterranean climate), named BNZEB (Benevento Nearly Zero-Energy Building).

2. Case Study and Method

2.1. Case Study Building: BNZEB

Figure 1A shows the BNZEB, outcome of an Italian project named "SMARTCASE" developed under the umbrella of the European Regional Development Fund. The net conditioned area is 70 m^2, the window/wall ratio is 22.5%, and the surface-to-volume ratio is equal to 1.03 m^{-1}.
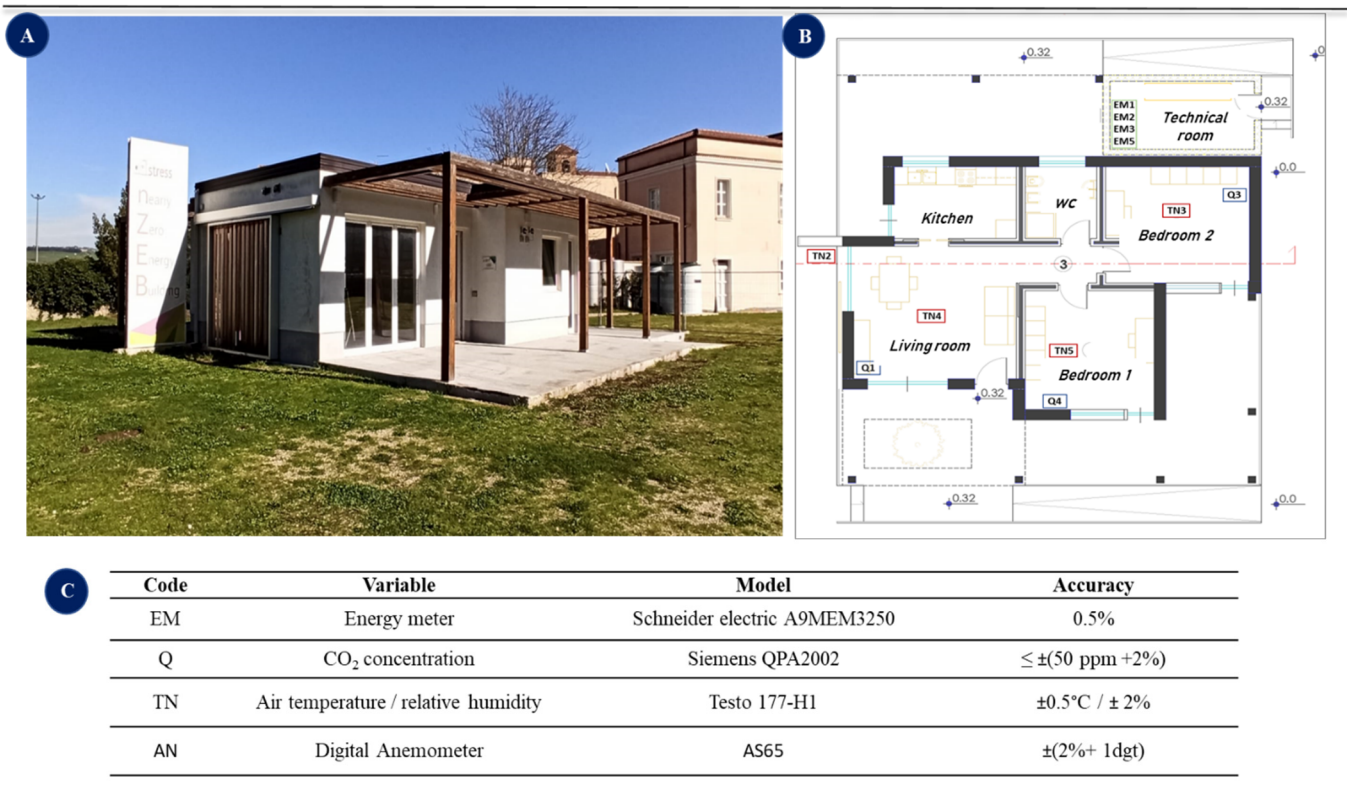
Figure 1. BNZEB: (A) external view, (B) layout, and (C) accuracy of main sensors.

The BNZEB is, at the same time, a research laboratory, suitable for testing and measuring energy, and indoor and outdoor conditions, but also a dwelling in which a comfortable life is allowed. In addition, as it has a small size, the BNZEB can be considered representative of a new design method aimed at reducing, as much as possible, the adoption of active systems and covering all of its energy needs entirely with available on-site renewable sources. The size does not influence the type of proposed analysis, which is contextualized to the type of occupation and external conditions.

The detailed design phase [47] and in situ characterization [48] have already been described by the authors, but some details are summarized here to improve the readability. Herein, it was also demonstrated that the building is classified as a nearly zero-energy one according to Italian standards; thus, it has the best energy class, and more than 50% of the energy consumed in the building is covered by on-site renewable production.

The BNZEB has been built in a west-facing area of the University of Sannio, in Benevento (lat. 41°7′55″, long. 14°46′40″, elevation 135 m), which is inside the Italian climatic zone "C", characterized by 1315 heating degree-days (baseline 20 °C). Benevento has a typical Mediterranean climate, characterized by warm to hot, dry summers and mild to cool, wet winters.

Cross-laminated wood makes up the structural frame, and it is coupled with two layers of fiber-wood insulation, with an overall thickness of 33 cm for the external walls, and about 50 cm for the roof. The measured thermal transmittance is equal to 0.19 W/m^{2}K and 0.22 W/m^{2}K, respectively, for the wall and the roof. Double-glazing systems with low-emissivity treatment and polyvinyl chloride frame are installed. The measured thermal transmittance for the window glass is 1.5 W/m^{2}K.

The layout is almost a square (Figure 1B), with the main entrance in the living room (22 m^2), a kitchen with openings to the north-west, and west exposures and two bedrooms. The living room, oriented south-west, has two large windows, one of which (5.8 m^2), on the south exposure, is permanently shaded by the wooden porch. The second window (5.3 m^2), on the west exposure, has an external shading system (Figure 1A) made of vertical

wooden slats that can be automatically moved by means of a temporal program or by means of the monitored incident radiation. Bedroom 1 has two windows with an internal white curtain. One of these is a smart window (1.7 m^2), but during the monitoring, it was clear all of the time; the other one has a net surface area of 2.1 m^2. Bedroom 2 (Figure 1B) has two windows (2.4 m^2 and 2.1 m^2) shaded by a white curtain and by the porch; this room borders the technical room on the north side.

For the heating and cooling needs, there are two systems. The first one is an aerothermal heat pump with a nominal heating power of 3.18 kW and cooling power of 2.14 kW. It provides hot water, heating, cooling, dehumidification, and mechanical ventilation, with an active thermo-dynamic heat recovery. The second one is a direct expansion heating/cooling system with two internal units. Moreover, to improve the overall performance of the HVAC system, a pre-treatment section for the outdoor ventilation air has been added. In detail, a heat exchanger may pre-cool the ventilation air during the summer period and pre-heat it during the winter before it reaches the aerothermal heat pump. The intermediate water-to-water heat exchanger is linked alternately to a horizontal ground-to-water heat exchanger or a solar collector. The horizontal geothermal probes (earth-to-water heat exchanger) are positioned at a depth of 2 m, with a total linear length of 100 m. The solar thermal collector (2.16 m^2) is also used for the domestic hot water stored in a tank (196 L). Finally, a photovoltaic system is installed on the roof. This is composed of 16 monocrystalline silicon panels, each with an area about 1.63 m^2 and a peak power of 330 Wp. The photovoltaic (PV) modules are oriented to the south (i.e., azimuth angle of 0°) with a tilt angle of 5°. Moreover, there is a lithium battery of 6.5 kWh for electricity storage.

2.2. Methodology

This study is organized in two main sections aimed at evaluating the indoor comfort condition with different approaches. The wintertime investigation is based only on the results of a monitoring campaign performed from November 2019 to January 2020, and it is aimed at evaluating the effect of different setpoint temperatures when the heat pump is operating in heating and ventilation mode with the intermediate heat exchanger turned off. On the other hand, during the summertime, different possible configurations for the HVAC systems are monitored during July in order to calibrate a numerical model of the building; this energy model is used for establishing the most adequate configuration to meet the comfort conditions. In both seasons, the building energy balance will be discussed considering the monitored values.

All information about the energy consumption, the generation from renewable sources, and the indoor microclimate conditions, like air temperature and relative humidity, have been collected with a time step of 15 min. The sensors available in the building have been adopted (see Figure 1B), and their accuracy is reported in Figure 1C.

To carry out the measurement campaign, air temperature and relative humidity sensors were installed in each room at 1.1 m (the head-height for a man sitting for typical studying work) near the table of the living room and kitchen and near the desks in the bedrooms. This does not always mean they are in the center of the room, but rather in a representative position with respect to the position mainly occupied by the students. At the center of the room, a globe-thermometer (emission equal to 0.95 and diameter of 15 cm) is positioned, and also an air temperature and relative humidity sensor (1.1 m), as well as the anemometer. The measurement of globe temperature with knowledge of the air temperature allows us to obtain the mean radiant temperature starting from a non-linear equation.

The monitoring campaign is performed in real operational conditions, when the building is occupied during the weekdays by two students from 9:00 to 18:00. For a complete analysis, the carbon dioxide (CO_2) concentration has been continuously monitored by the sensors located in each room. However, it is not discussed, because it was verified that for all configurations and setups the CO_2 concentration is 500 ppm above the outdoor

concentration, as required by considering the category II of comfort in residential buildings according to the EN 15251 standard [49].

2.2.1. Wintertime Investigation

During the wintertime, the monitoring campaign is based on the application of the adaptive theory for establishing the setpoint value for the air temperature starting from the monitored value of the outdoor temperature. The base rule for the adaptive comfort is a linear equation, $T_c = a \cdot T_{ext} + b$, where T_c is the expected indoor comfort temperature, T_{ext} is the outdoor reference temperature, a indicates the degree of adaption, and b is the y-intercept [50]. The a and b values are different for each adaptive thermal comfort model, and these are usually found by means of experimental data. Starting from the study of Dear and Brager [51], the ANSI/ASHRAE 55:2004 has included the adaptive model in the reference comfort standard; the standard was updated in 2020. In the same year, ISSO 74 was adopted in Netherlands [52], and revised in 2014. Later, in 2007, the new European standard EN 15251 was introduced, and updated by UNI EN 16798-1 [53]. Most recently, it was introduced in China [54]. The following table summarizes the main equations proposed in the mentioned standard. In the table, T_{ext} is usually calculated starting from the daily mean external air temperature (t_{ed}) for a time d of a series of equal intervals (day). In its equation, α is a constant ranging between 0 and 1, and in some cases, it is recommend to use 0.8. For the standard ANSI/ASHRAEE and in the case of UNI EN 16798-1, only the optimal expected indoor comfort temperature is reported; instead, the first standard provides two ranges for T_c, namely 80% and 90% acceptability, and in the second case, an upper and lower limit of category are provided. For the other two models, equations of the normal level of expectation are considered (this category refers to the design of new buildings or to substantial renovation).

According to the reference standard, the proposed equations can be applied only to occupant-controlled naturally conditioned spaces. Only in the case of beta spaces (ISSO 74) can the model be used for centrally controlled environments in the summer period.

Thus, the application of the adaptive theory for the wintertime is worthy of investigation. Moreover, it is also proposed for the selected case study because the building is characterized by a high level of insulation, and it is interesting to evaluate if the thermal-hygrometric conditions are comfortable when the setpoint temperature is different from the threshold value (20 °C) indicated by the Italian standards [55]. The proposed approach is based on a linear equation, as seen in the models summarized in Table 1. In particular, the setpoint temperature (T_{set}) has been fixed according to an empirical relation reported in Equation (1). It is calculated taking into account the reference outdoor temperature (T_{ext}):

$$T_{set} = 20 \pm a * T_{ext} \tag{1}$$

Herein, a is the adaptation coefficient that ranges, arbitrarily, between 0 and 0.15, and T_{ext} is the average value of the external temperature recorded during the seven days preceding the one to be heated. The equation indicates that for finding the setpoint, a factor that is a function of external conditions can be added or subtracted to the reference value of 20 °C. This approach is different from the models proposed in Table 1, where starting from the reference external temperature, a minimum comfort temperature is added or sometimes subtracted.

Table 1. Equations of adaptive models from literature.

ANSI/ASHRAE 55: 2010 [51]	$T_c = 0.31 \cdot T_{ext} + 17.8$ $T_{ext} = (1-\alpha) \cdot [t_{ed-1} + \alpha \cdot t_{ed-2} + \alpha^2 \cdot t_{ed-3} + \alpha^3 \cdot t_{ed-4}$
UNI EN 16798-1:2019 [53]	$T_c = 0.33 \cdot T_{ext} + 18.8$ $T_{ext} = (1-\alpha) \cdot [t_{ed-1} + \alpha \cdot t_{ed-2} + \alpha^2 \cdot t_{ed-3} + \alpha^3 \cdot t_{ed-4} + ..]$
ISSO 74:2014 [52]	**ALFA spaces** $Upper\ limit \begin{cases} T_c = 0.33 \cdot T_{ext} + 18.8 + 2 & 10\,°C \le T_{ext} \le 25\,°C \\ T_c = 24 - 5 & °C \le T_{ext} < 10\,°C \end{cases}$ $Lower\ limit \begin{cases} T_c = 0.2 \cdot T_{ext} + 18 & 10\,°C \le T_{ext} \le 25\,°C \\ T_c = 20 - 5 & °C \le T_{ext} < 10\,°C \end{cases}$ $T_{ext} = 0.2 \cdot [t_{ed-1} + 0.8 \cdot t_{ed-2} + 0.8^2 \cdot t_{ed-3} + 0.8^3 \cdot t_{ed-4} + ..]$ **BETA spaces** $Upper\ limit \begin{cases} T_c = 24 - 5 & °C \le T_{ext} < 10\,°C \\ T_c = 0.33 \cdot T_{ext} + 18.8 + 2 & 10\,°C \le T_{ext} \le 16\,°C \\ T_c = 26 & 16\,°C < T_{ext} \le 25\,°C \end{cases}$ $Lower\ limit \begin{cases} T_c = 0.2 \cdot T_{ext} + 18 & 10\,°C \le T_{ext} \le 25\,°C \\ T_c = 20 - 5 & °C \le T_{ext} < 10\,°C \end{cases}$ $T_{ext} = 0.2 \cdot [t_{ed-1} + 0.8 \cdot t_{ed-2} + 0.8^2 \cdot t_{ed-3} + 0.8^3 \cdot t_{ed-4} + ..]$
GB/T 50785:2012 [54]	$Cold\ climates \begin{cases} T_c = 0.73 \cdot T_{ext} + 15.28 & 18\,°C \le T_{ext} \le 28\,°C \\ T_c = 0.91 \cdot T_{ext} - 0.48 & 16\,°C \le T_{ext} \le 28\,°C \end{cases}$ $Hot\ and\ mild\ climates \begin{cases} T_c = 0.73 \cdot T_{ext} + 12.72 & 18\,°C \le T_{ext} \le 30\,°C \\ T_c = 0.91 \cdot T_{ext} - 3.69 & 16\,°C \le T_{ext} \le 28\,°C \end{cases}$ $T_{ext} = (1-\alpha) \cdot [t_{ed-1} + \alpha \cdot t_{ed-2} + \alpha^2 \cdot t_{ed-3} + \alpha^3 \cdot t_{ed-4} + ..]$

However, it should be noted that this relation has not been found in the literature or in the international standards, and it is not validated. The proposed analysis is the first attempt to verify the effectiveness of changing the setpoint temperature in a building designed to be very insulated and with a high contribution of solar gains during the winter. After this step, a deeper work will be done with the aim of validating the equation, while also considering different types of occupation.

Based on the monitored data, the most used thermal comfort indices have been calculated with the aim of comparing a quantitative variable with the occupants' subjective judgment. In particular, the predicted mean vote (PMV) and the predicted percentage of dissatisfied (PPD) are evaluated according to the definition proposed in [56] in two representative rooms at different times: 10:00, 13:00, and 17:00. The analysis is reported for the living room, representative of high solar gains during the winter, and Bedroom 1.

Moreover, an hourly energy balance is performed, and some assessment indices are discussed for evaluating the incidence of the renewable electricity source. The first index (RenEl) is the ratio between the amount of electricity from a renewable source used to satisfy the request and the total daily consumption of the building. The second one (PV$_{in}$) is the ratio between the generation from the PV system and the daily consumption. The last one is the Load Match Index, defined in Equation (2). It quantifies the ability to temporally match a building's load and the in situ energy generation, and thus it indicates the ability to work beneficially with respect to the needs of the grid infrastructure.

$$F_{loadmatch} = \frac{1}{N} * \sum_p \min\left[1, \frac{g(t)}{l(t)}\right] \tag{2}$$

In more detail, $g(t)$ is the on-site electricity generation, $l(t)$ is the load, and t is the time interval (e.g., hour, day, or month). Meanwhile, p is the evaluation period, and N is the

number of data samples (i.e., if p is equal to 1 year, this value is 12 for a monthly time interval and 8760 for an hourly time interval, respectively).

2.2.2. Summertime Investigation

The summertime investigation starts from a previous work of the authors, where it was demonstrated that the coupling of a ground-to-water heat exchanger with the two available cooling systems had great potential to achieve the nZEB target, with reference to the energy requirement for space cooling [57]. Instead, in this paper, the effect of the HVAC configurations, reported in Table 2, on indoor comfort conditions is evaluated by means of numerical simulations with EnergyPlus [58] though the DesignBuilder v.6.0 interface [59].

Table 2. Information about tested HVAC configurations.

Conf.	Monitoring Period	People Presence and Thermal Load	Ventilation System	Pre-Cooling Activation	Cooling System	Indoor Setpoint
C1	8–11 July	Yes	Packaged heat pump	Off	Packaged heat pump	25 °C
	12 July	No				
C2	15–18 July	Yes	Packaged heat pump	On	Packaged heat pump	25 °C
C3	22–25 July	Yes	Packaged heat pump	On	Direct Expansion heat pump	25 °C
C4	27–28 July	No	Packaged heat pump	Off	Direct Expansion heat pump	25 °C
	29–30 July	Yes				

The numerical model of the BNZEB has been already created and calibrated in another work [48], but for the purpose of the present study, it has been upgraded, also using a new version of the software interface. The numerical simulation needs a weather file as input. In this case study, it was defined with outdoor data monitored on the roof of the building during the same days during which the energy balance is evaluated and the indoor conditions are monitored. This procedure allows evaluation of the calibration indices for reliable internal and external forcing. In more detail, the meteorological datasets contain climatic data with hourly frequency based on measurements of the external air temperature and relative humidity, the global horizontal radiation, the wind speed, and direction, and so on.

The calibration of the numerical model has been performed according to the methodology proposed by M&G Guidelines [60]. The statistical indices are the Mean Bias Error (MBE), Equation (3), and the Coefficient of Variation of Root Mean Square Error (CvRMSE), Equations (4)–(6).

$$MBE = \frac{\sum_p (S - M)_{daily}}{\sum_p M_{daily}} \qquad (3)$$

$$RMSE = \sqrt{\sum \frac{(S - M)_{daily}^2}{N_{interval}}} \qquad (4)$$

$$A_{hourly} = \frac{\sum_p M_{interval}}{N_{interval}} \qquad (5)$$

$$CvRMSE\,(\%) = \frac{RMSE_{period}}{A_{period}} * 100 \qquad (6)$$

In the equations: S is the simulated data, M is the measured data, and N is the number of sampling. Obviously, the lower the value of these indicators, the better the quality and the predictive capacity of the numerical model.

The calibrated model is used for a CFD (Computational Fluid Dynamics) analysis aimed at verifying the thermal comfort indicators at some critical points. The CFD technique is used for the analysis of the heat transfer by following these two steps:

- discretization of the governing differential equation using numerical methods;
- solving of the discretized version of equation with high-performance computers.

Unlike an energy simulation that gives results in which the investigated variables assume different values over time (i.e., hourly results), before running a CFD simulation, a precise time instant must be fixed. In this study, CFD simulations are carried out in the days reported in Table 1, and the results will be shown for three different times, that is, 10:00, 14:00, and 18:00.

CFD analysis is a space-variant analysis. The calculation method requires that the geometric space across which the calculations are conducted is firstly divided into a number of non-overlapping adjoining cells, which are collectively known as the finite volume grid (or mesh). The grid used by DesignBuilder CFD is a non-uniform rectilinear Cartesian grid, and the adopted grid has been generated with 0.15 m grid spacing.

The equations are solved considering the 2-k-ε turbulence model that involves replacing the instantaneous velocity in the Navier–Stokes and energy equations with a mean and fluctuating component. The calculation process involves replacing the defining set of partial differential equations with a set of finite difference equations. The upwind scheme has been used. It allows the convective term to be calculated assuming that the value of the dependent variable at a cell interface is equal to the value at the cell on the upwind side of the interface.

In more detail, 2D distributions of indoor air temperature and 3D distributions of PPD and PMV inside the building will be shown.

In this season, the energy balance between the generation from the PV system and the overall energy consumption allows us to understand the potential daily energy saving and the best management strategy for the trade-off between the energy requirements and production.

3. Results

3.1. Wintertime Assessment Results

In this section, firstly, the characterization of thermo-hygrometric conditions inside the building during the wintertime is discussed; subsequently, the energy consumption and the energy balance are shown. During this period, the air-to-air heat pump provides temperature control and mechanical ventilation with an internal filter that purifies the air before supplying it into the building. That system is also provided with active thermodynamic heat recovery, and this means that part of the exhaust air interacts with the outdoor heat exchanger (evaporator in winter), so that the thermal level of the ambient air is more suitable to discharge or supply energy. Another part of return air is recirculated, mixed with primary (outdoor) air, filtered again, and handled in the packaged heat pump before the new supply into the rooms.

3.1.1. Indoor Comfort Analysis by Means of Measured Variables

Figure 2 shows the monitored values of relative humidity inside and outside the building for the considered periods with variable setpoint temperatures (indicated in the orange boxes), taking into consideration the living room and Bedroom 1 for the first week. These trends allow us to conclude that the setpoint temperature does not influence the value of relative humidity, which varies between 30% and 60% in both rooms; it seems mainly influenced by the outdoor value and its interaction with the recirculated flow. In more detail, considering 12 January and 8 December, when the setpoint is 20 °C and the outdoor relative humidity varies respectively from 48% to 87% and 62% to 96%, in the living room, the recorded values vary between 35% and 42% in January (with lower outdoor values) and between 46% and 56% in December.

Figure 2. Relative humidity trend: (**A**) setpoint lower that 20 °C and (**B**) upper 20 °C.

The influence of solar gains on the humidity value is also notable. Indeed, considering the same days between 12:00 and 15:00, in the living room there is a sensible increment of the indoor temperature and a decrement of the relative humidity. In this time interval, the maximum solar gains are achieved, and during 12 January, the temperature passes from 18.3 °C to 21.4 °C, and the indoor humidity from 41% to 36%. Similarly, during 8 December, the temperature goes from 19.8 °C to 21.4 °C, and the indoor humidity from 54% to 50%.

Moreover, when the setpoint is increased (14 January, 20.8 °C) and the outdoor relative humidity is comparable to the 12 January (48–85%), the indoor value varies from 33% to 39%, as in the case of a setpoint of 20 °C. The same observation can be made for 12 December, with a lower setpoint.

Figure 3A reports the monitored air temperature during 7–13 December. In this period, the external temperature varies in the range between 4 °C and 14 °C, and in all days, the temperature monitored in the bedroom is more uniform. It is some tenths higher than the living room value, and thus closer to the setpoint. It is due to the higher percentage of glazed surfaces in the living room. Even by using a setpoint lower than 20 °C, the temperature inside the building is within 17.5 °C and 19.5 °C. Only in some conditions, when the solar radiation gives an important contribution, does the air temperature rise up to the setpoint value. For instance, during 11 December, the setpoint is 18.7 °C, but inside the living room, during the afternoon, the sensor recorded 21.6 °C. However, the occupant perception is not positive for this management strategy, because they have described the indoor condition as "slightly cold" for all days.
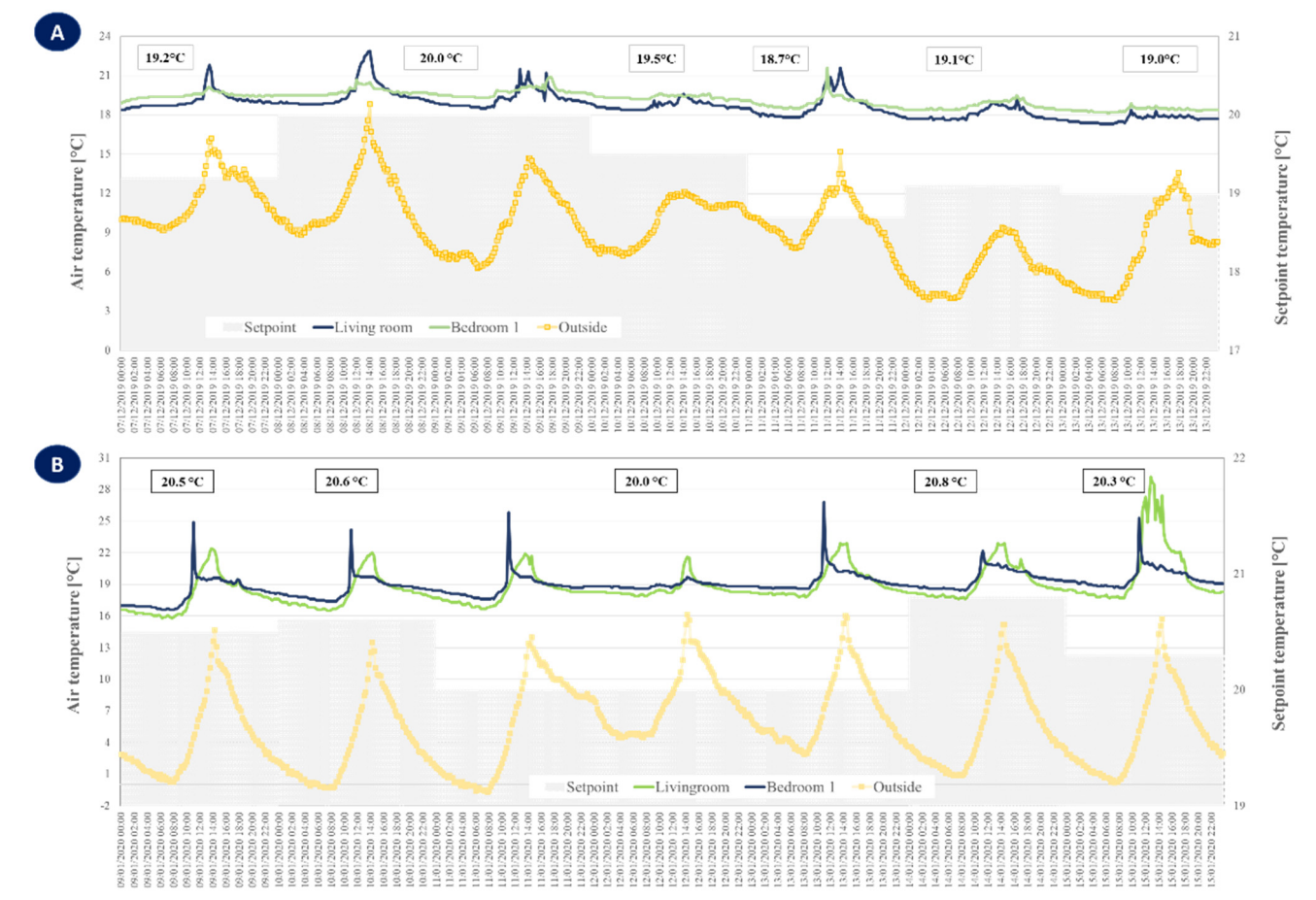
Figure 3. Air temperature trend: (**A**) setpoint lower that 20 °C and (**B**) upper 20 °C.

In the period 9–15 January, the setpoint was increased; meanwhile, the outdoor temperature varied between 0 °C and 14 °C. For all days, the value of the air temperature is usually lower than the setpoint, except during the afternoon, when in the living room the temperature rises up 20 °C, with a maximum value of 28 °C during 15 January that is characterized by a solar radiation (monitored on the roof) of around 400 W/m^2.

It is interesting that when the outside temperature decreases during the night, the temperature inside the building drops about two degrees, even if the setpoint is settled at 20 °C. For these days, the occupants have affirmed they are in comfort conditions. This is a notable conclusion that underlines how the occupants are influenced by the knowledge of the test to which they are subjected, and how the comfort has a significant psychological component. Indeed, it can be objectively observed that the indoor trends of the two periods are comparable.

This conclusion is also supported by comparison of the temperature trend in three days with extreme setpoints: 9 December, 11 December, and 14 January. Indeed, with 20 °C and mild external conditions (09/01, outdoor temperature from 6.3 °C to 14.7 °C) in the living room, the temperature ranges between 18.5 and 21.5 °C, with the maximum value at 14:00, when there is the maximum outdoor temperature and the solar radiation on south wall; in Bedroom 1, this range is 19.3–20.9 °C (maximum at 11:45). For comparable outdoor conditions (11/01, outdoor temperature from 5.6 °C to 15.2 °C) and the lowest setpoint, the temperature varies between 17.6 °C and 21.6 °C, with maximum value at 14:00 in the living room, and between 18.4 °C and 21.6 °C (maximum at 12:00) in Bedroom 1. Finally, with the higher setpoint and extreme variable conditions (14/01, outdoor temperature from 0.9 °C

to 15.2 °C), in the living room the recorded temperature varies between 17.6 °C and 22.9 °C (maximum at 13:30), and in Bedroom 1 between 18.4 °C and 22.2 °C (maximum at 11:15).

Two main conclusions can be found. Firstly, the design of glazed elements assures comparable peak values of indoor temperature during the early afternoon when the setpoint temperature is different, and thus it seems to be the main force of the energy balance. Secondly, for the case study, the solar contribution mainly regards the window on the south-west exposure of the living room (in the early afternoon); meanwhile, the designed porch reduces the effect of solar gains on the south window during the late morning. Instead, Bedroom 1 receives the benefits of solar radiation during the late morning.

Table 3 shows the value of the comfort indices calculated with the monitored values during the days with occupants. These have been calculated according to the model proposed in [56] with the implementation of the equations for PMV and PPD in a mathematical sheet. Herein, the measured parameters are used as input data as explained in the previous section. The metabolic rate of individuals in this study was assumed to be uniform at 1.1 met (corresponding to work office); winter clothing resistance of 1 clo was also assumed.

Table 3. PMV and PPD calculated indices.

		PMV (%)	PPD (%)	PMV (%)	PPD (%)
		Living Room		**Bedroom**	
	10:00	−0.5	10.2	−0.3	6.9
9 December 2019	13:00	−0.3	6.9	−0.3	6.9
	17:00	−0.2	5.8	−0.1	5.2
	10:00	−0.6	12.5	−0.4	8.3
10 December 2020	13:00	−0.5	10.2	−0.4	8.3
	17:00	−0.6	12.5	−0.4	8.3
	10:00	−0.7	15.3	−0.5	10.2
11 December 2019	13:00	−0.4	8.3	−0.5	10.2
	17:00	−0.5	12.5	−0.5	10.2
	10:00	−0.8	18.5	−0.6	12.5
12 December 2019	13:00	−0.7	15.3	−0.5	10.2
	17:00	−0.6	12.5	−0.5	10.2
	10:00	−0.8	18.5	−0.6	12.5
13 December 2019	13:00	−0.8	18.5	−0.6	12.5
	17:00	−0.8	18.5	−0.6	12.5
	10:00	−1.3	40.3	−1.3	40.3
9 January 2020	13:00	−0.6	12.5	−0.9	22.1
	17:00	−0.9	22.1	−0.8	18.5
	10:00	−0.9	22.1	−0.8	18.5
10 January 2020	13:00	−0.2	5.8	−0.5	10.2
	17:00	−0.6	12.5	−0.5	10.2
	10:00	−0.9	22.1	−0.7	15.3
13 January 2020	13:00	−0.2	5.8	−0.5	10.2
	17:00	−0.7	15.3	−0.6	12.5
	10:00	−0.5	10.2	−0.4	8.3
14 January 2020	13:00	0.0	5.0	−0.3	6.9
	17:00	−0.4	8.3	−0.4	8.3
	10:00	−0.6	12.5	−0.4	8.3
15 January 2020	13:00	0.0	5.0	−0.2	5.8
	17:00	−0.3	6.9	−0.3	6.9

Considering the obtained results, for the bedroom, the PMV values are not really different in the considered weeks, with a presumable opinion of "slightly cold", except during 9 January, which is really cold according to the calculated indices. Considering the living room, during 9 December, 11 December, and 14 January, the analytical calculation of the PMV and PPD indicates comparable conditions, with a setpoint of 20 °C or higher (14 January). The main difference is at 13:00, but this is attributable to the direct solar radiation and not to the heating system; indeed, at this time, the HVAC is turned off, because in both days the setpoint has been exceeded. In Bedroom 1, the indices for 9 December are even better than 14 January. Instead, when the lower setpoint is set, the conditions are more critical in both rooms, but these are quite acceptable according to [51,52,57], since the PMV is 0.5. The values in the living room, once again, underline the important role of solar gains. Indeed, in the morning the heating system is not able to meet comfort conditions, but at 13:00, the comfort indices indicate pleasant conditions, comparable to the other days. When the sun has set, the living room is colder, and the PPD is higher than the threshold value.

When the setpoint is 18.7 °C, at 10:00, the living room seems to be more comfortable according to PMV, and this happens also at 17:00; on the other hand, during the early afternoon at 13:00, the higher setpoint causes only 5.8% of people to be dissatisfied and results in a lower value of 8.3%. However, in both cases the indoor conditions could be considered acceptable. Regarding the external conditions, the solar radiation monitored both on vertical and horizontal surfaces was higher during 13 January. This condition may have contributed to different occupants' perception.

More generally, the proposed analysis suggests that the occupants, in their environmental assessment, are affected both by the external weather conditions and by the knowledge of the test being carried out. Indeed, the second week was characterized by an average value of solar radiation higher than the considered week in December, and the sky was usually clear. Probably, this condition led the occupants to consider the rooms more comfortable, due to the solar gains, and also because the indoor temperatures were comparable. Moreover, it can be remarked that when the room is characterized by large glazed surfaces, the contribution of solar radiation also allows one to balance the indoor conditions when a low setpoint is considered. For the case study, the temperature inside the room can exceed the setpoint by even more than 3 °C. The proposed data suggest that for reducing the heating demand in highly insulated buildings, the setpoint can be decided starting from the external conditions, but it could be better to take into account the solar radiation and not only the air temperature for the formulation of an analytical relation for the setting.

3.1.2. Building Energy Balance from Monitored Data

The impact of the selected setpoint on the energy balance can be found in Figure 4; it reports the monitored daily energy consumption for both selected weeks. The overall energy consumption and the separated contributions of the main loads are plotted. The slight difference is attributable to the energy consumption for the monitoring system (sensors and computer) with which the BNZEB is equipped.

The results show that the HVAC system covers around 63–72% and 72–85% of the total building energy consumption, respectively, for the first and second week. The artificial lighting accounts for around 2% of the overall energy consumption. The analysis is not easy, and it needs to consider the global external conditions. For 11 December and 13 January, with comparable outdoor temperature and relative humidity (e.g., average daily temperature respectively of 7.2 °C and 6.9 °C), the adoption of a lower setpoint assures a reduction of heating consumption of 43%, while also maintaining comfortable conditions according to the previous analysis. On the other hand, when the comparison is done with 9 December, characterized by milder external conditions, the reduction is 17%. In this case, the heating demand is influenced by lower heat losses and high solar gains during the day, with a setpoint of 20 °C, and thus the benefit of the adoption of 18.7 °C is

lower. Considering 8 January, with an average daily temperature of 6.7 °C and minimum and maximum peak values of 3 °C and 14 °C, the heating consumption increases by 65%, passing from 20 °C to 20.3 °C, and it is more than three times higher than the case with 18.7 °C.
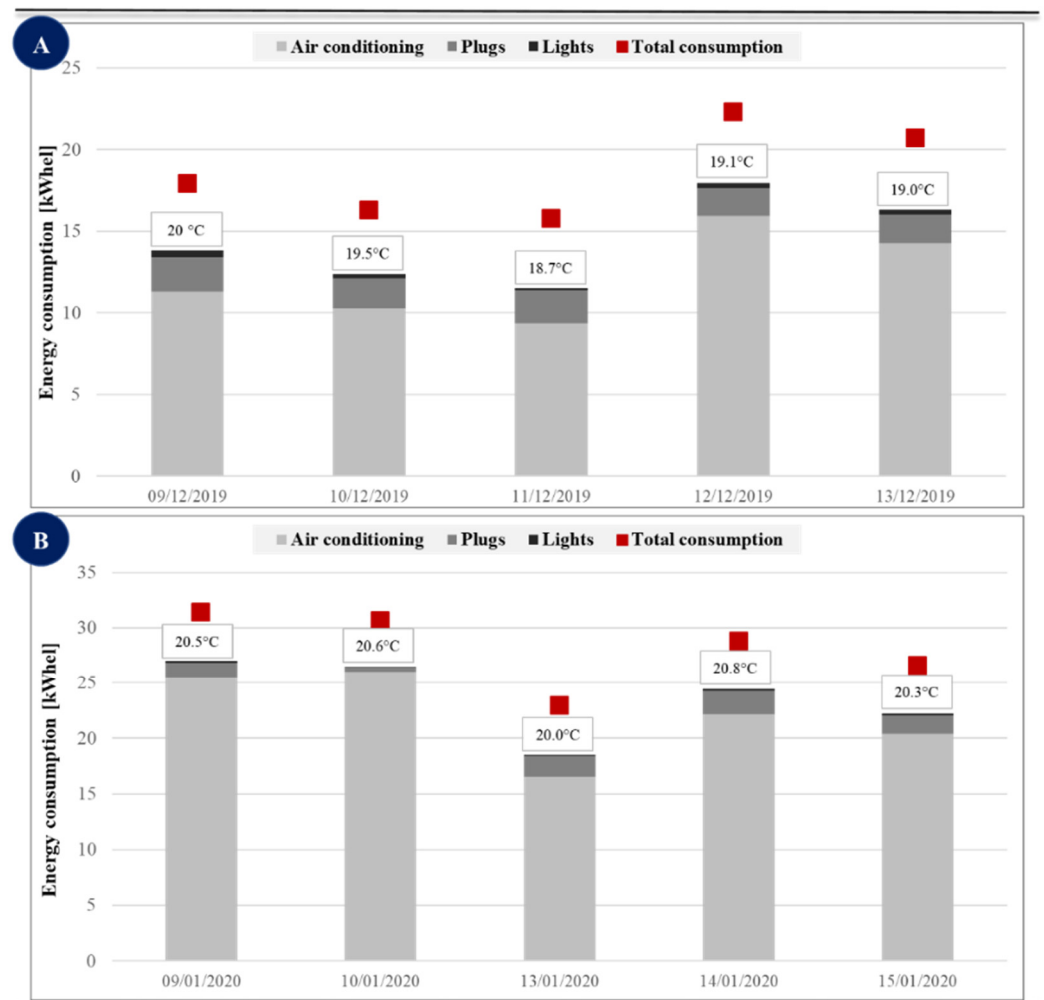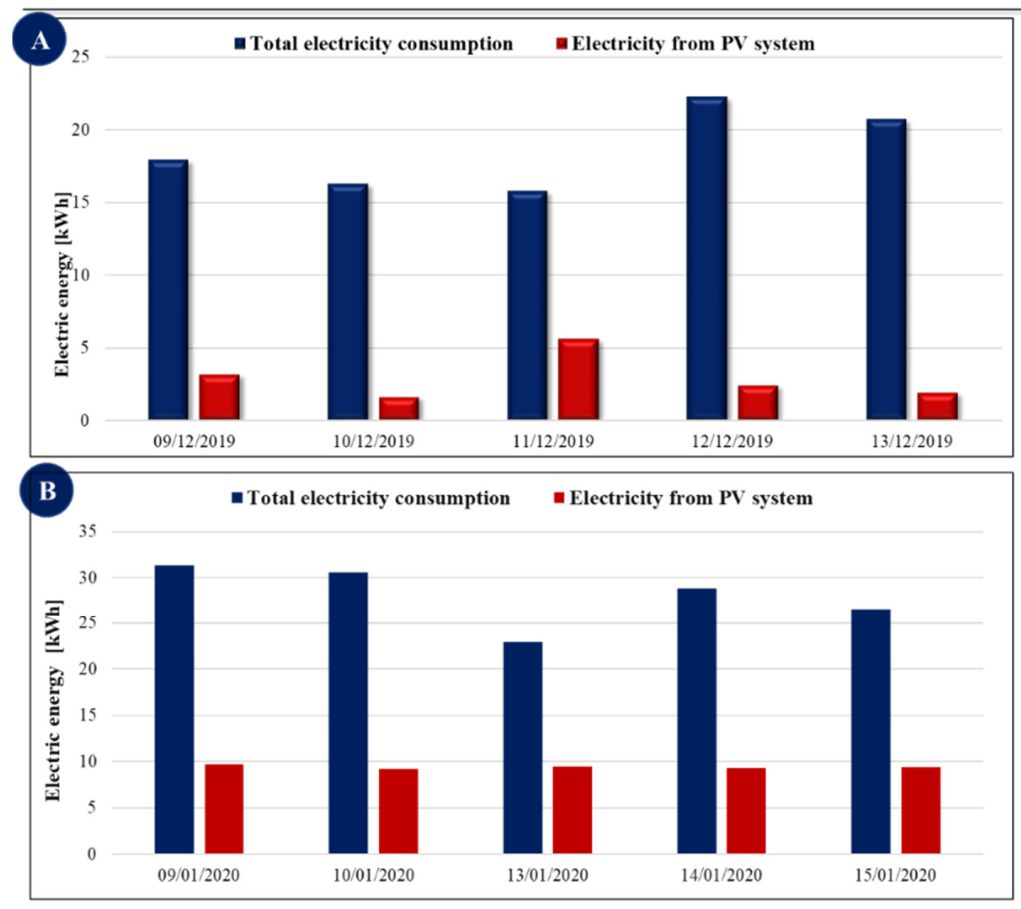

Figure 4. Energy consumption trend: (**A**) setpoint lower that 20 °C and (**B**) upper 20 °C.

The variation of the energy consumption cannot be charged only to the adopted setpoint; the evaluation of external conditions that can positively (solar gains) or negatively (heat losses due to colder conditions) influence the heating request is also important. For instance, considering 13 December, with 19.0 °C as setpoint and an average daily temperature of 7.3 °C, if the comparison is done with 9 December (mild climate, average daily temperature of 9.7 °C), it is found that the heating request increases by 26%; if it is compared with 13 January instead, the heating request is lower by around 14%.

These data, based not on simulations but on monitoring of real conditions, confirm that the management strategy of the heating system has a great influence on the building's energy balance. However, the adopted strategy can be decided taking into consideration, dynamically, the external conditions for reaching the energy-saving and the thermal comfort objectives.

Figure 5 shows the daily energy balance considering the electric energy consumption and the generation from the PV system. Table 4 reports the introduced hourly indices.

Figure 5. Daily energy balance between energy consumption and PV generation: (**A**) setpoint lower that 20 °C and (**B**) upper 20 °C.

Table 4. Hourly indices regarding energy balance.

	RenEl	PV$_{in}$	F$_{loadmatch}$
9 December 2019	17.8%	17.8%	17.4%
10 December 2019	10.1%	10.7%	11.21%
11 December 2019	35.8%	35.8%	34.8%
12 December 2019	12.0%	11.0%	10.9%
13 December 2019	9.28%	9.28%	8.73%
9 January 2020	30.9%	30.9%	35.7%
10 January 2020	30.1%	30.1%	36.2%
13 January 2020	41.2%	41.2%	52.0%
14 January 2020	32.3%	32.3%	39.1%
15 January 2020	35.4%	35.4%	48.4%

During the winter period, the renewable electricity generation cannot satisfy the energy need of the building, and the selected setpoint does not significantly change the balance. Indeed, the RenEl indicates that the renewable energy used for the electricity request cannot reach 50% during the analyzed days. More generally, the comparison of RenEl and PV$_{in}$ indicates that thanks to the energy storage, the used renewable energy coincides with the production in almost all days. This testifies that the BNZEB has been designed to maximize self-consumption, but the production is usually lower than the expected, and for this reason the building requires for more time using electricity from the energy grid. The Load Match Index results are within 11% and 56%, and thus the

percentage of electrical demand covered by on-site generation at the hourly level is very low.

There is not a unique interpretation for the incidence of the adopted setpoint. Indeed, the effect on the renewable integration requires us to take into consideration the global external conditions. Globally, the first considered week was cloudier that the second one, and this justifies the lower value of the indices if the adopted setpoints were lower. In more detail, for 11 December and 13 January, also with comparable conditions, it is not possible to compare the results. Indeed, during both days, all produced electricity has been used by the building (RenEl is equal to PV_{in}), but thanks to higher solar radiation on the roof, the production during 13 January is almost double compared to 11 December; thus, the results seem better than the case with the lower setpoint. However, 11 December, with the lowest setpoint, is characterized by a higher percentage of integration during the first selected week, and this is due to both the lower consumption and the higher production of all other days.

In the second considered week, the producibility of the PV system is comparable in all days; thus, some comparisons can be made. Looking at 13 January, with the lower setpoint, it is characterized by the maximum integration, since the renewable production (9450 Wh) can satisfy 41.2% of the consumption, and the match between the request and the production is higher than in the other cases (52%). With a comparable production (9415 Wh) and a setpoint of 20.3 °C, the integration becomes 35.4%.

The proposed data indicate that it is difficult to establish a relation between the utilization of renewable in situ production and the adopted setpoint, because the production is related to the solar radiation captured by the panels, which is a variable that does not influence the needs of the building. However, when the renewable production is comparable, a decimal variation of the adopted setpoint greatly influences the integration rate.

Based on the obtained results, it can be concluded that the external temperature monitored in the days before the setting could be used for deciding the setpoint in a high-performance building. However, the solar radiation in the most glazed room should be used for selecting the management strategy. The analytical evaluation of comfort parameters demonstrates that there is not a notable variation in the people dissatisfied, and the integration of renewable adoption can be increased if the external conditions are not favorable.

Other tests are needed for evaluating the incidence of external conditions on the occupants' perception.

3.2. Summertime Assessment Results

As explained in the methodological section, four different configurations of HVAC system were tested and compared by means of simulations as well as monitoring results.

3.2.1. Simulation Analysis of Indoor Comfort Conditions

The simulation model has been verified for the variables that are used during the CFD investigations. The output of simulations performed in all different configurations were compared in terms of indoor air temperature and relative humidity with the measured data. Table 5 shows the evaluated indices for the air temperature and the relative humidity in Bedroom 1 (Figure 1B). The results are always within the admitted tolerances; in particular, the M&G Guidelines [60] require for the MBE a value ≤ 10% and for the CvRMSE ≤ 30% when the validation is performed with hourly data. All indices are below the threshold value provided by [60]; thus, the model can be considered well calibrated and well representative of the real conditions inside the building for all configurations.

Table 5. HVAC system configurations and corresponding calibration indices for one building room.

|	HVAC System		MBE (%)	CvRMSE (%)	MBE (%)	CvRMSE (%)	Evaluation Period
	Cooling System	Pre-Cooling Activation	Air Temperature		Relative Humidity		
C1	Heat pump	Off	−1.55	3.11	5.94	11.56	8–12 July
C2	Heat pump	On	1.86	−1.91	−7.79	10.74	15–18 July
C3	DX system	On	−3.66	−1.87	−6.38	8.95	22–25 July
C4	DX system	Off	3.04	3.08	0.23	5.91	27–30 July

The calibrated numerical model of the building has been used with the purpose of investigating the air temperature and the distribution of global comfort indices by means of the CFD tool of DesignBuilder. In more detail, before running the simulation, all boundary conditions have been fixed by using the measured values for surface and window temperatures, HVAC supplies, extracts, and so on. In the various rooms, the cooled air is introduced by means of vents, which are reproduced by boundary-defining conditions such as the minimum velocity of the air jet, the supply temperature, the supply angle, and the flow rate; then, the air is extracted by extraction vents. Moreover, CFD calculations have been performed by selecting the values for metabolic rate and clothing thermal resistance of 1 met (light-intensity activity) and 0.5 clo for the clothing insulation (a typical summer value), respectively.

Table 6 shows the selected days and the indication of the HVAC configuration. During these days, the setpoint temperature inside the building is 25 °C, and the simulations are carried out at three different times, that is, 10:00, 14:00, and 18:00. Table 5 shows the values of external temperature and the average indoor temperature for each day.

Table 6. Investigated hours: outdoor temperature and average indoor temperature.

HVAC Configuration and Investigated Day	Investigated Hours	Outdoor Temperature (°C)	Average Indoor Temperature (°C)
C1—12 July	10:00	27.9	24.5
	14:00	31.9	24.9
	18:00	24.2	24.1
C2—17 July	10:00	26.6	25.1
	14:00	38.7	24.6
	18:00	33.6	24.3
C3—24 July	10:00	31.3	24.3
	14:00	37.9	24.8
	18:00	39.5	24.5
C4—30 July	10:00	27.6	24.2
	14:00	33.6	24.4
	18:00	30.7	24.1

Considering 12 July, at 10:00, Figure 6A shows the 2D distribution of the indoor air temperature; the 3D distributions of PPD and PMV inside the building are reported in Figure 6B,C, respectively. The distribution of indoor air temperature varies around the real average indoor value indicated in Table 6.
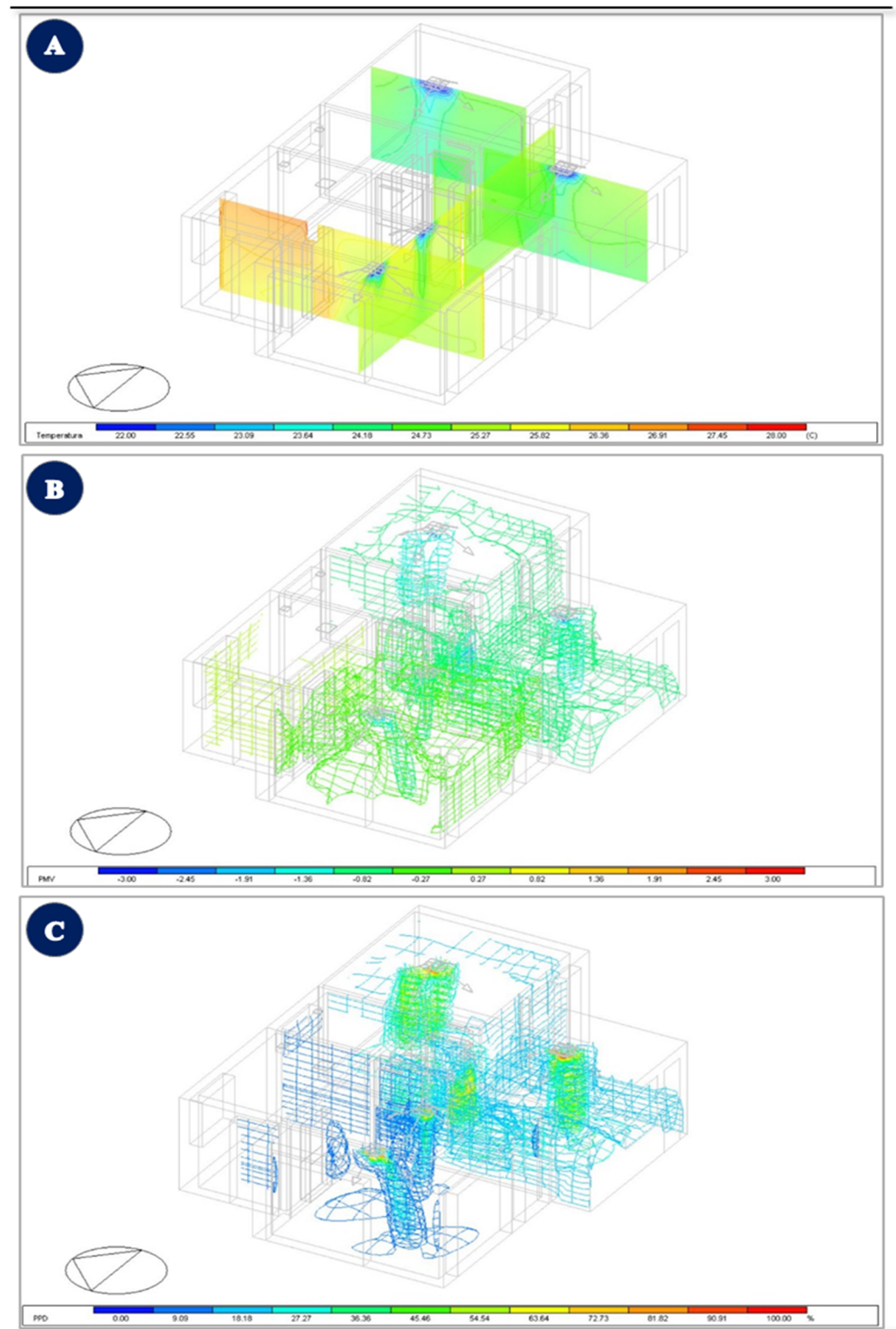
Figure 6. CFD results on 12 July at 10:00: (**A**) air temperature 2D distribution; (**B**) PMV and (**C**) PPD 3D distribution.

In particular, the bedrooms are characterized by rapid temperature equalization, mainly in Bedroom 2, which is disadvantaged in terms of solar gains due to the prevalent exposure. As indicated in Figure 6B, the temperature distribution in Bedroom 1 determines a "slightly cold" sensation, according to PMV distribution, except at the vent where the air volume is associated with a cold flow, which corresponds (Figure 6C) to a PPD higher than

the threshold value of 10% [59]. The punctual value of these indices in the room center at a height of 1.1 m (man sitting at a table) is reported in Table 7 for the coldest (Bedroom 2) and the hottest (kitchen) rooms and for the living room. The PPD is 20%, and this indicates that without the contribution of inner and solar gains, the temperature of the supply air is low for Bedroom 2. This could be maintained in comfort conditions with a higher setpoint and thus lower cooling consumption.

Table 7. PMV and PPD values calculated on 12 July.

12 July	Bedroom 2			Kitchen			Living Room		
	10:00	**14:00**	**18:00**	**10:00**	**14:00**	**18:00**	**10:00**	**14:00**	**18:00**
Operative temperature (°C)	24	23.7	23.6	26.4	26.2	25.5	25.2	26.3	25.3
PMV (%)	−0.83	−0.94	−0.98	0.05	−0.03	−0.28	−0.39	0.01	−0.36
PPD (%)	20	24	25	5	5	7	8	5	8

In the living room, the cold flow is neutralized by the solar gains and the volume assumes a higher temperature mainly near the windows, despite the presence of two vents. Figure 6B also indicates that the PMV is near a judgment of "slightly warm" in correspondence of the vents; indeed, as reported in Table 7, the PMV is 8%. The selected setpoint and the diffusion strategy are adequate for balancing the solar gains in the morning.

The kitchen is characterized by a higher level of temperature due to the absence of cooling vents, which also causes a stratification of the air due to a lack of significant convective flows and air speed. In this room, according to PMV and PPD (Table 6), the conditions are acceptable and more adequate than the other rooms.

Figure 7 shows the 2D distribution of air temperature inside the BNZEB, resulting from two CFD simulations concerning 12 July at 14:00 and 18:00, when the outside mean temperature was 31.9 °C and 24.2 °C, respectively.

At both times, the bedrooms are characterized by lower and more uniform values of temperature, and the path of the cold air introduced by the HVAC to the floor is also evident, mainly in Bedroom 2. The solar radiation, due to the two south-facing windows in Bedroom 1 and in the living room, enters inside the room, and it causes an increment of the air temperature. In the living room, the temperature is even higher than in Bedroom 1, despite the presence of two vents that provide cooled air. The kitchen is the hottest room of the dwelling, due to the absence of cooling vents, which also causes air stratification. However, according to values reported in Table 6, the indoor sensation complies with the comfort standard, except in the morning.

The values of PPD and PMV (Table 7) confirm that Bedroom 1 should be managed with a different setpoint, because the percentage of dissatisfied persons increases until it reaches 25% in the evening, and thus the room could also assure comfortable conditions without the active system due to effect of thermal inertia and lower inner solar gains during the night. On the other hand, the supply conditions (flow rates and temperature) are optimal for the living room, where the PPD is also always lower than 10% during the early afternoon when the solar radiation is incoming. The shading system is able to intercept the radiation; thus, the design of BNZEB seems to be adequate for reducing the overheating problem.

Figure 8 reports the 2D distributions of air temperature during 17 July. These values are the result of CFD simulations when the HVAC configuration was C2, and thus the heat pump worked to provide cooled air, and the ventilation air was pre-cooled by crossing the water-to-air heat exchanger.
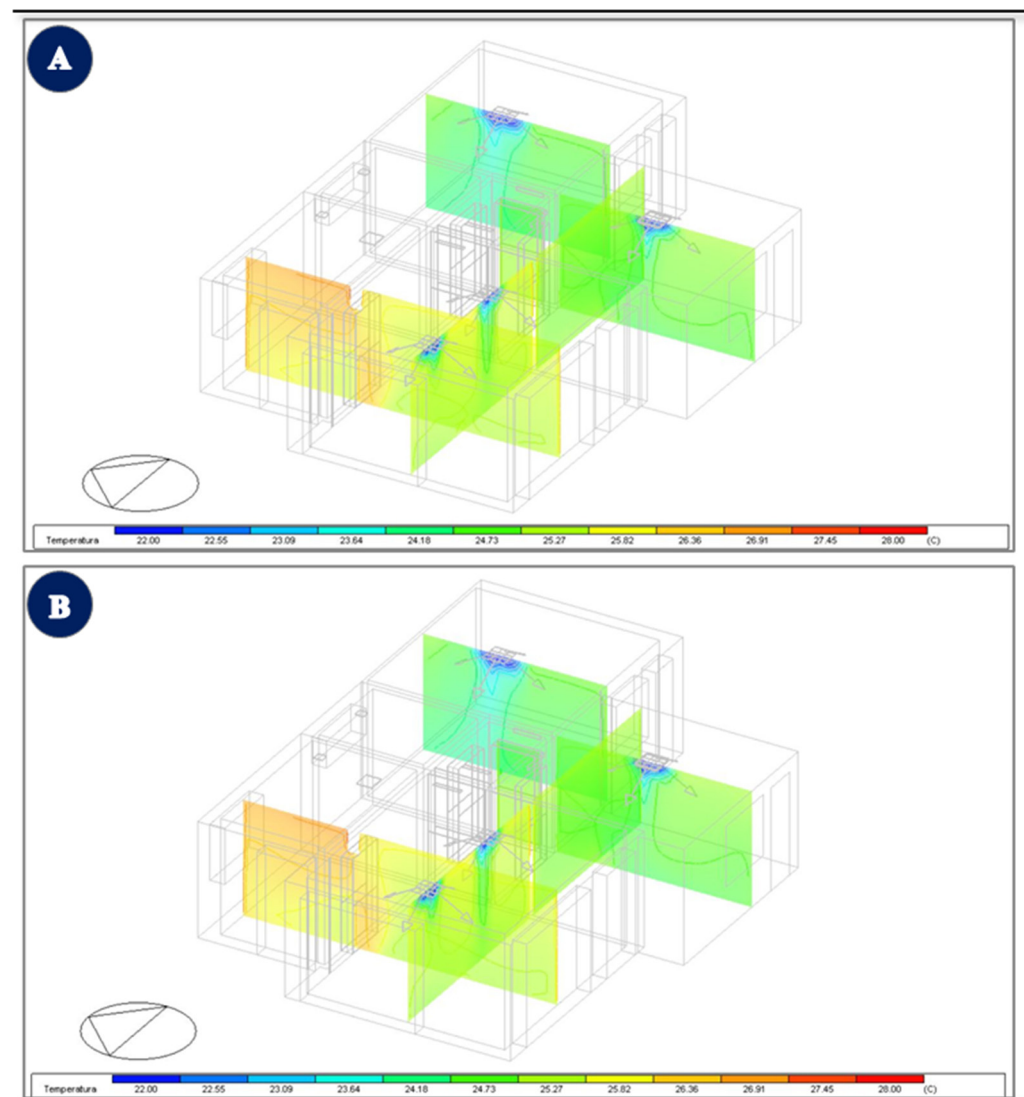
Figure 7. 2D distribution of air temperature on 12 July: (**A**) 14:00 and (**B**) 18:00.

The temperature on 17 July was warmer than 12 July, with a maximum temperature of 38.7 °C compared to 32 °C, but with comparable global solar radiation of 670 W/m^2 and 617 W/m^2, respectively. These conditions have led to comparable temperature distributions for both HVAC configurations. However, in this case, it can be noted that the bedrooms have more comparable conditions, and assuming as reference the PMV and PPD calculated for Bedroom 2 (see Table 8), a cold feeling could be experienced in the morning, with perfect conditions in the other investigated hours. In comparison with configuration C1, the living room is characterized by higher values of temperature; the temperature difference between the center surface and the window is around 6 °C. Thus, if the PPD is also lower than 10% in the afternoon and evening, considering the center of the room, some local discomfort phenomena could occur near the glazed surfaces. The kitchen, during the three considered hours, is characterized by a higher level of temperature compared to 12 July, due to both the absence of cooling ceiling diffusers and to the adjacency to the living room. Even in these cases, there is a stratification of the air in the kitchen. However, the comfort indices (Table 8) indicate that the room has acceptable conditions in the afternoon and evening.
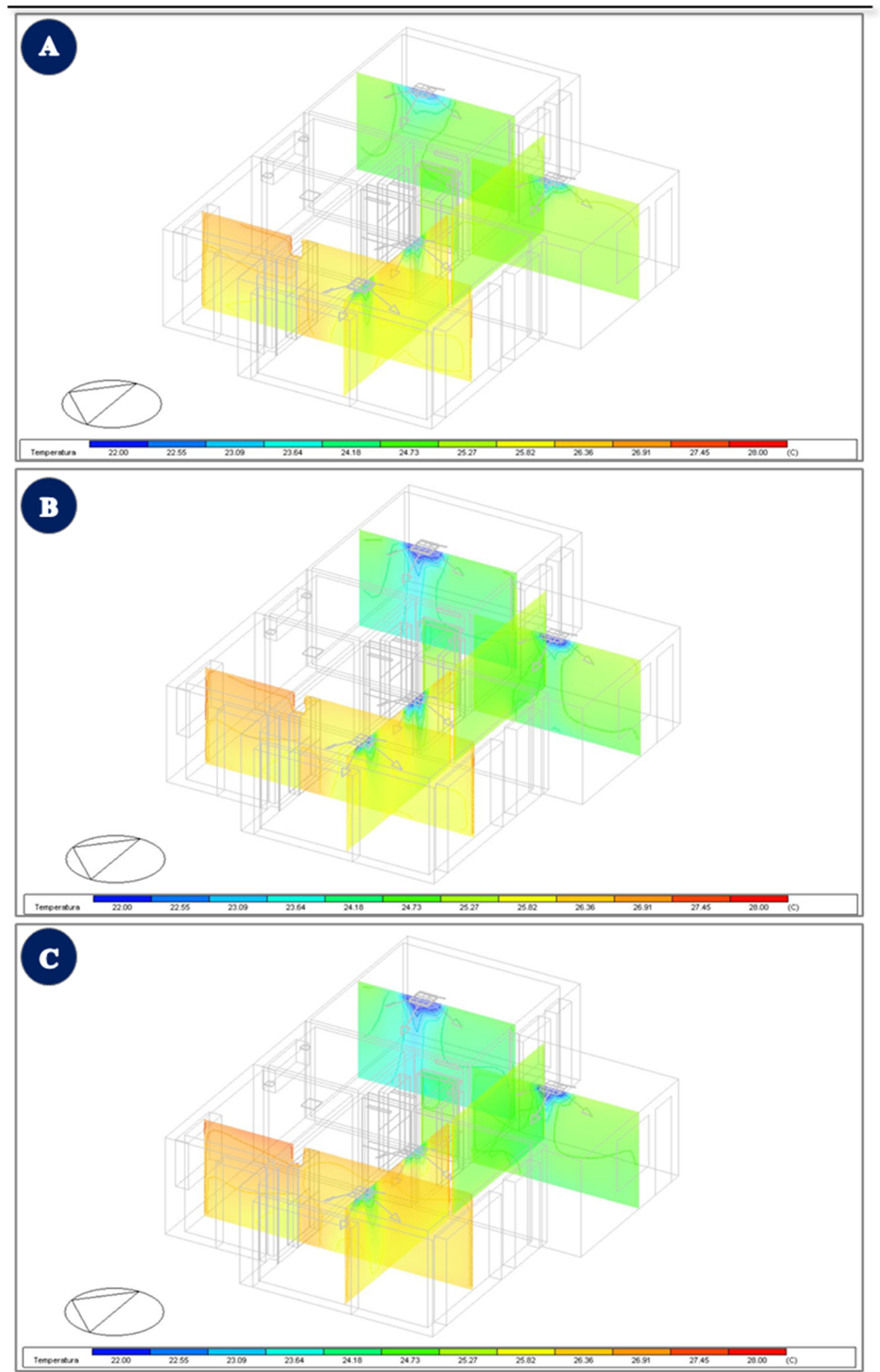
Figure 8. 2D distribution of air temperature on 17 July at (**A**) 10:00, (**B**) 14:00, and (**C**) 18:00.

Table 8. PMV and PPD values calculated on 17 July.

17 July	Bedroom 2			Kitchen			Living Room		
	10:00	**14:00**	**18:00**	**10:00**	**14:00**	**18:00**	**10:00**	**14:00**	**18:00**
Operative temperature (°C)	24.3	26.4	26.0	24.0	26.7	26.3	24.1	26.8	26.4
PMV (%)	−0.72	0.05	−0.1	−0.83	0.16	0.01	−0.80	0.19	0.05
PPD (%)	16	5	7	20	6	5	18	6	5

Briefly, the temperature profiles and the calculated indices are comparable to the previous case, and thus it can be concluded that considering thermal comfort, the pre-handling of the ventilation air does not make significant differences. What happens in terms of energy consumption has to be evaluated.

Moreover, it can be underlined that the selected setpoint as well as the temperature and flow rate of HVAC are suitable for the management of indoor conditions when the outdoor conditions are very warm. Starting from the temperature distribution until 10:00, for reducing the consumption without compromising the indoor comfort, it is probably possible to operate with a higher setpoint or supply conditions. The findings about the kitchen are also interesting; indeed, thanks to the designed architectural distribution, the selected glazed surfaces and the building's thermal mass assure comfortable conditions without direct cooling.

In Figure 9, the 2D distributions of air temperature inside the BNZEB are shown during 24 July for the selected hours. In these cases, the HVAC configuration was C3, and thus the heat pump worked only to provide ventilation, while the backup DX multi-split system worked to supply cooled air, and the outdoor air was pre-cooled by crossing the water-to-air heat exchanger.

At 14:00, the living room is the warmer room, but globally, the temperature distribution indicates lower values than 17 July, and the PPD is 6%. In this case, the supplied cold air is able to neutralize the effect of solar gains, and the more uniform distribution suggests that local discomfort phenomena should not occur. Bedroom 2 is the coldest room, and considering that the PPD is 25% both in the morning and in the evening, it is clear that less cold supply air could be used, or a lower flow rate.

According to Figure 9, Bedroom 1 is less affected by solar gains compared to the living room, and the temperature distributions are comparable in the three hours as reported in Table 9.

Table 9. PMV and PPD values calculated on 24 July.

24 July	Bedroom 2			Kitchen			Kitchen		
	10:00	**14:00**	**18:00**	**10:00**	**14:00**	**18:00**	**10:00**	**14:00**	**18:00**
Operative temperature [°C]	23.6	25.2	23.6	24.1	25.4	24.8	24.3	25.7	25.0
PMV [%]	−0.98	−0.39	−0.98	−0.80	−0.32	−0.54	−0.72	−0.21	−0.47
PPD [%]	25	8	25	18	7	11	16	6	10

Finally, in Figure 10 the 2D distributions of air temperature inside the BNZEB are shown for 30 July when the heat pump worked only to provide ventilation, while the backup DX multi-split system worked to supply cooled air. The outdoor conditions are similar to 12 July, with temperature variation between 20.0 °C and 33.6 °C, and maximum solar radiation of 622 W/m². In addition, during this day, it is clear that the average indoor temperature is lower compared to those obtained with C1 and C2 (12 and 17 July).
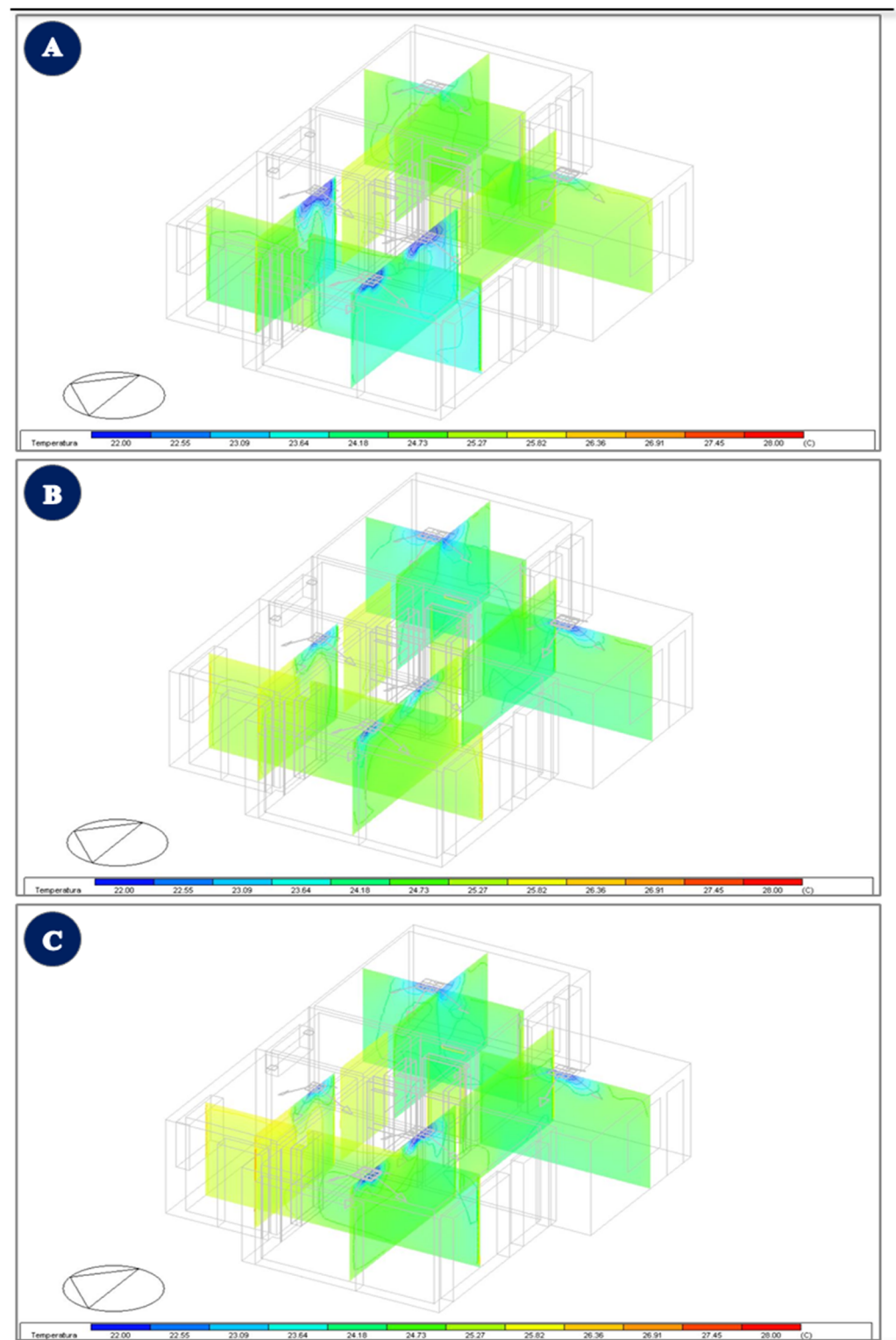
Figure 9. 2D distribution of air temperature on 24 July at (**A**) 10:00, (**B**) 14:00, and (**C**) 18:00.
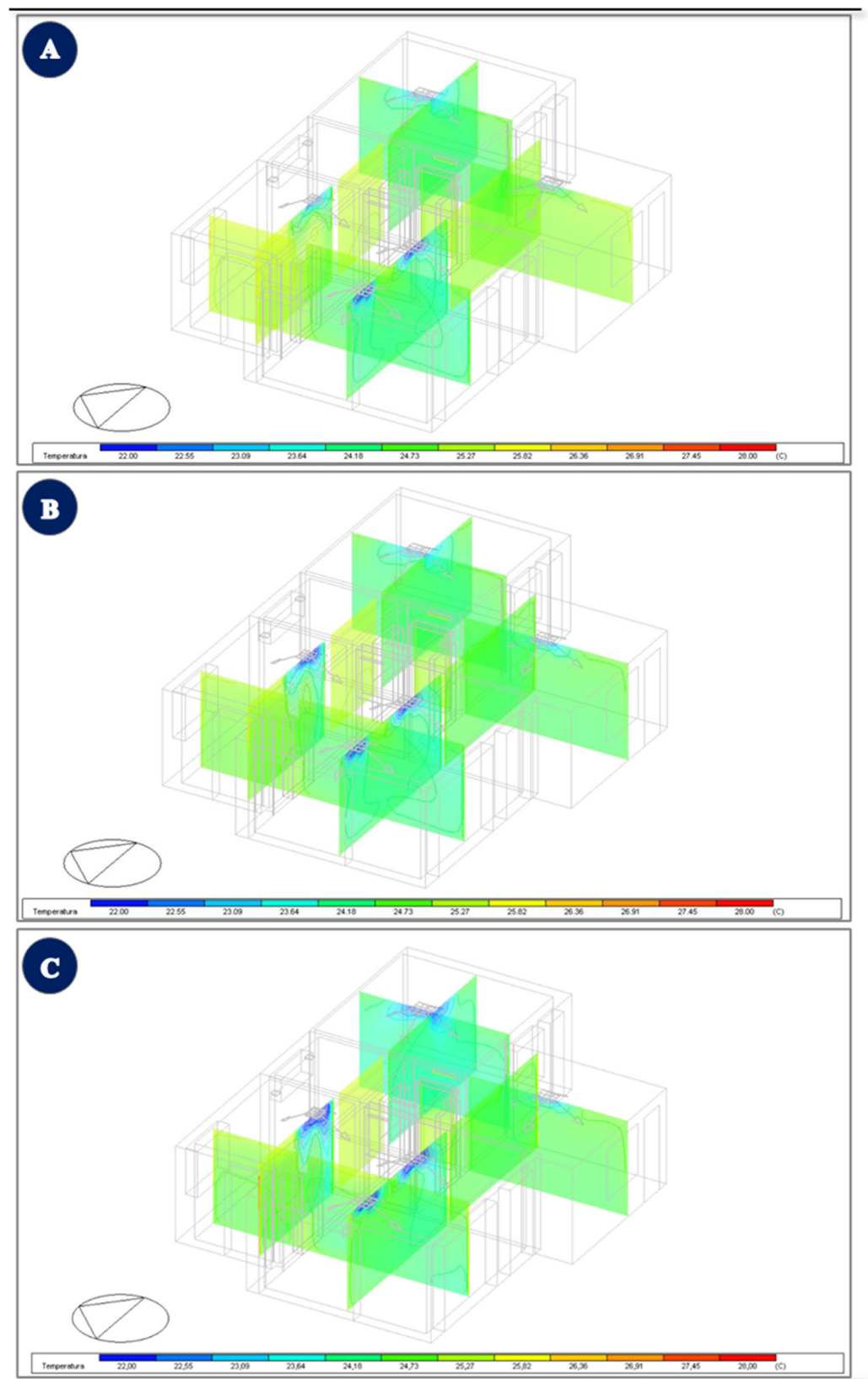
Figure 10. 2D distribution of air temperature on 30 July at: (**A**) 10:00, (**B**) 14:00, and (**C**) 18:00.

In more detail, Bedroom 2 is always the coldest room, due to its exposure and supplied air. In the living room, the management of HVAC system assures uniform and slightly cold conditions, which is also due to the induced cooling effect by the vent of the kitchen. The hottest room in these cases is also the kitchen, where due to the cooling vent, there is no stratification of the air; however, at the most critical time (14:00), the PPD is 8%. Really, the indoor conditions are quite uniform in the whole building, but at the most favorable times, the perceived sensation would be slightly cool, and this means that the cooling system provided too much cooled air. Detailed results are reported in Table 10.

Table 10. PMV and PPD values calculated on 30 July.

30 July	Bedroom 2			Kitchen			Living Room		
	10:00	14:00	18:00	10:00	14:00	18:00	10:00	14:00	18:00
Operative temperature (°C)	24	25.4	24	24.2	25.2	24.2	24	25.3	24
PMV (%)	−0.83	−0.32	−0.83	−0.76	−0.39	−0.76	−0.83	−0.36	−0.83
PPD (%)	20	7	20	17	8	17	20	8	20

In general, the monitoring results coupled with the CFD analysis have indicated that in the summertime as well, the management of the HVAC system could be decided with a dynamic approach based on the outdoor conditions. Indeed, for buildings such as the BNZEB with good passive control of indoor conditions, the supply variables and the setpoint could be changed during the day following the variation of outdoor temperature and solar radiation. Moreover, the analysis suggests that in residential buildings as well, the indoor comfort could benefit from adoption of differentiated microclimate control in each room. When the building envelope is designed with bioclimatic criteria, each room is characterized by different conditions during the day, and thus, higher energy savings could be obtained with an adaptive regulation system.

The CFD analysis performed according to the four different configurations allowed us to verify that the pre-handling system has no effect on the indoor comfort. Indeed, it only guarantees a lower temperature of the air supplied to the heat pump; therefore, a saving of the energy demand and costs are expected, while the supply temperature, operated by the A/C vents, does not change. Moreover, it can be noticed that during the summertime, the pre-handling of the ventilation air, based on air pre-treatment, does not make substantial differences in terms of indoor comfort, or in terms of energy consumption.

3.2.2. Building Energy Balance from Monitored Data

Figure 11 shows the daily energy balance, and thus the electricity consumption, the generation from PV system, and the electricity available in the battery. Table 11 reports the calculation of the introduced hourly indices for evaluating the incidence of production from the photovoltaic system at a smaller time scale.

Globally, it can be found that the most convenient configuration is C4, because in each day the energy consumptions are lower than the other configurations. A further optimization is also possible according to the CFD analysis, because the DX system could be managed with a higher setpoint or higher supply temperature with a reduction of the energy consumption. Instead, the comparison between C1 and C2 highlights that the adoption of the heat pump requires the integration of a pre-handling unit to be convenient in terms of energy request.
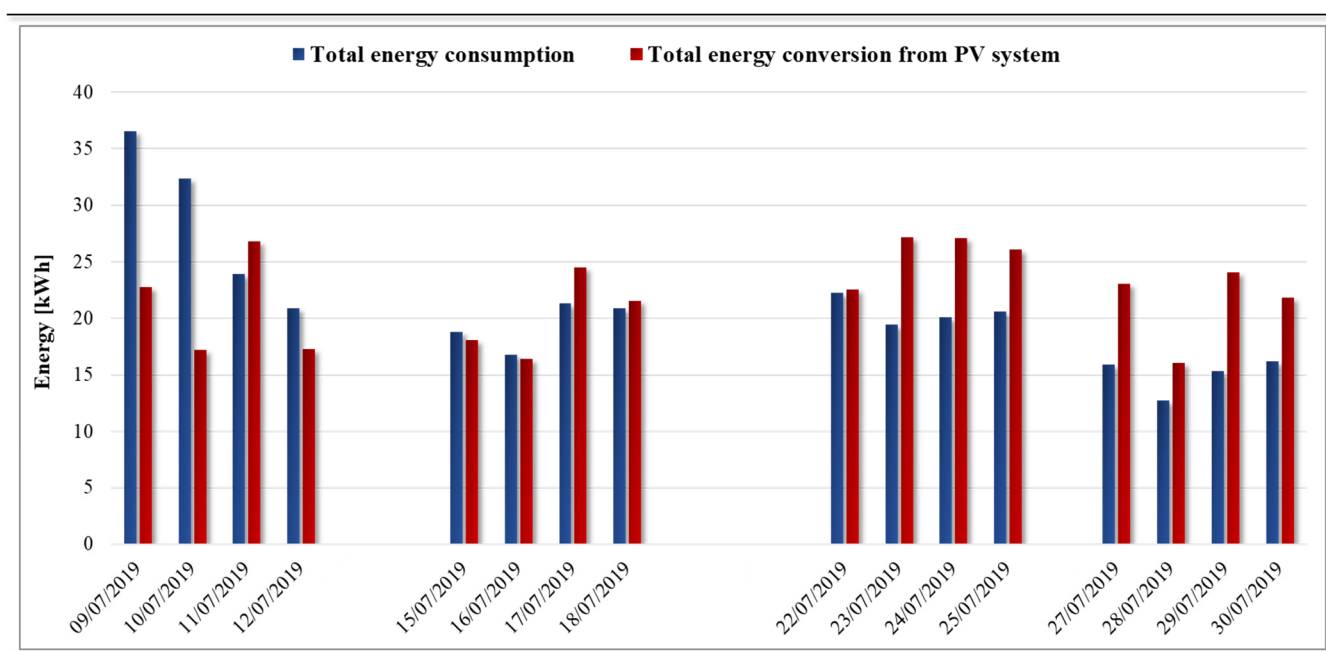
Figure 11. Daily energy balance between energy consumption and PV generation.

Table 11. Hourly indices concerning energy balance in the building.

	RenEl (%)	PV (%)	$F_{load\ match}$ (%)
9 July	63.0	62.5	60.9
10 July	57.0	53.3	50.4
11 July	85.7	111.8	61.8
12 July	80.4	82.60	54.2
15 July	81.9	96.3	60.5
16 July	86.4	97.8	73.6
17 July	95.5	114.8	90.8
18 July	80.4	103.0	56.8
22 July	80.9	101.3	72.2
23 July	81.6	139.8	72.4
24 July	89.2	135.2	81.1
25 July	85.3	126.3	75.0
27 July	87.2	145.0	79.5
28 July	85.8	126.3	84.2
29 July	95.4	156.6	91.8
30 July	95.7	134.8	92.1

With regard to the renewable production, the PV_{in} index is always high and, starting from 17 July, it is always more than 100%, meaning that the PV production, from 16 to 27 kWh/day, exceeds the daily electricity demand of the building. This value does not indicate that the energy request is completely covered by the generation from the PV system as represented through the RenEl index, which is between 56% to 97%. This finding is important. Indeed, with a monthly or daily approach, it could be said that the renewable production is able to satisfy the entire energy demand of the building within the considered period. Instead, with a short timestep, the unbalance between the demand and the production and the importance of working on a more adequate management strategy for maximizing the matching on an hourly basis is clear. The indication of the load match for the case study by means of the $F_{load\ match}$ is quite satisfactory, being between 50% and 92%.

For a better understanding of these considerations, the days analyzed in terms of thermal comfort can be compared. The measures indicate that for 12 July, the energy consumption for air conditioning is 15.7 kWh, while, on 17 July, this is equal to 12.9 kWh, and thus about 18% lower. This result confirms that with the same indoor conditions and comparable thermal comfort indices, the pre-handling unit allows one to reduce the energy consumption. This finding is even more interesting taking into consideration that 17 July is characterized by warmer conditions. The configuration C2 also increases the matching between the renewable production and the energy demand, with the $F_{load\ match}$ that passes from 54% to 91%.

The comparison between 24 and 17 July, with comparable outdoor conditions, indicates that the C3 configuration is characterized by lower consumption (around 6%). The energy saving could be higher taking into consideration the findings of the CFD analysis. Indeed, with the DX system, the supply conditions or the setpoint can be set at a higher level without compromising the comfort, and this management action could assure lower requests. However, it is also important to understand that the configuration C2 guarantees higher integration of the renewable source. Indeed, despite the higher production of 24 July (PV equal to 135%), the $F_{load\ match}$ is 81%.

Moreover, the daily energy consumption of the configuration C3 is higher by around 46% compared to C4, considering 24 and 30 July. Although this result seems predictive of the inconvenience of the pre-handling system, it must be considered that 24 July has been characterized by more heavy external weather conditions than 30 July. This last day assures a higher load match (92%), and almost the entire energy demand (95.7%) is covered by in situ production.

The comparison between C1 and C4 suggests, again, that with comparable external conditions, the energy request of the DX system is lower (23%). Finally, for this case study, the configuration C4 is the best one from the points of view of both energy consumption and the load-matching problem. Different management of the DX system could increase this convenience.

4. Conclusions

Starting from monitored data in an nZEB in a Mediterranean climate during the wintertime, how the variation of the setpoint temperature affects the comfort conditions and the energy consumption was evaluated. The results are encouraging for further analysis. Indeed, it was found that energy savings (from 17% to 43%) are achievable by lowering the setpoint with respect to the Italian legislation threshold and through the utilization of on-site renewable electricity, which can be maximized during the day with the lowest productivity. The comfort indices suggest that the indoor conditions are also acceptable with lower setpoints, mainly when the room is characterized by a large glazed surface. However, the perception of people does not always agree with analytical evaluations; the judgment seems closely related to the external conditions, mainly in term of sky clearness.

Moreover, for the summertime, the CFD analysis indicates that the pre-handling system does not affect indoor comfort. It only guarantees a lower temperature of the air supplied to the heat pump, and therefore a saving of the energy demand and costs, but the supply temperature does not change. Globally, considering all available data, the most convenient configuration is the operation of the DX system with a reduction of energy consumption near 20%. In this case, management with a higher setpoint or higher supply temperature is also possible; this strategy can determine a further reduction of the energy consumption and the increment of load matching. Moreover, it was shown that although currently, the energy balances on nZEBs are usually based on annual or monthly data, what happens at lower scales of time (daily or hourly) should be considered, in order to have profitable designs oriented towards maximizing the self-consumption of energy production. This would assure economic profitability and a better interaction with the local grid infrastructure.

Obviously, all presented data are strictly related to the building application and to the climate zone under investigation. However, the adopted solutions and the learned results could be useful guidelines for building and system design in areas with similar boundary conditions, and thus climates, living styles, and construction types.

References

1. European Parliament. Directive 2010/31/EU of the European Parliament and of Council of 19 May 2010 on the energy performance of buildings (recast). *Off. J. Eur. Union* **2010**, *L153*, 13–35.
2. European Parliament. Directive 2018/844 of the European Parliament and of Council of 30 May 2018 on amending Directive 2010/31/EU on the energy performance of buildings and Directive 2012/27/EU on energy efficiency. *Off. J. Eur. Union* **2018**, *L156*, 75–91.
3. Chen, Y.; Lin, G.; Crowe, E.; Granderson, L. Development of a Unified Taxonomy for HVAC System Faults. *Energies* **2021**, *14*, 5581. [CrossRef]
4. Butera, F.M. Zero-energy buildings: The challenges. *Adv. Build. Energy Res.* **2013**, *7*, 51–65. [CrossRef]
5. Mor, G.; Cipriano, J.; Gabaldon, E.; Grillone, B.; Tur, M.; Chemisana, D. Data-Driven Virtual Replication of Thermostatically Controlled Domestic Heating Systems. *Energies* **2021**, *14*, 5430. [CrossRef]
6. Moon, J.W.; Han, S.H. Thermostat strategies impact on energy consumption in residential buildings. *Energy Build.* **2011**, *43*, 338–346. [CrossRef]
7. Ben-Nakhi, A.E.; Mahmoud, M.A. Application of building-dynamics-based control strategies to improve air-conditioning performance in educational buildings. *Adv. Build. Energy Res.* **2017**, *11*, 153–179. [CrossRef]
8. Kazanci, O.B.; Olesen, B.W. Beyond nearly-zero energy buildings: Experimental investigation of the thermal indoor environment and energy performance of a single-family house designed for plus-energy targets. *Sci. Tech. Built Environ.* **2016**, *22*, 1024–1038. [CrossRef]
9. Zalewska, M.E. The Impact of Incentives on Employees to Change Thermostat Settings—A Field Study. *Energies* **2021**, *14*, 5315. [CrossRef]
10. De Feijter, F.J.; van Vliet, B.J. Housing retrofit as an intervention in thermal comfort practices: Chinese and Dutch householder perspectives. *Energy Effic.* **2021**, *14*, 1–18. [CrossRef]
11. Haniff, M.F.; Selamat, H.; Khamis, N.; Almin, A.J. Optimized scheduling for an air-conditioning system based on indoor thermal comfort using the multi-objective improved global particle swarm optimization. *Energy Effic.* **2019**, *12*, 1183–1201. [CrossRef]
12. Guillén-Lambea, S.; Rodríguez-Soria, B.; Marín, J.M. Comfort settings and energy demand for residential nZEB in warm climates. *Appl. Energy* **2017**, *202*, 471–486. [CrossRef]
13. Reda, F.; Pasini, D.; Laitinen, A.; Teemu, V. ICT intelligent support solutions toward the reduction of heating demand in cold and mild European climate conditions. *Energy Effic.* **2019**, *12*, 1443–1471. [CrossRef]
14. Katafygiotou, M.C.; Serghides, D.K. Indoor comfort and energy performance of buildings in relation to occupants' satisfaction: Investigation in secondary schools of Cyprus. *Adv. Build. Energy Res.* **2014**, *8*, 216–240. [CrossRef]
15. Ghahramani, A.; Zhang, K.; Dutta, L.; Yang, Z.; Becerik-Gerber, B. Energy savings from temperature setpoints and deadband: Quantifying the influence of building and system properties on savings. *Appl. Energy* **2016**, *165*, 930–942. [CrossRef]
16. Tzivanidis, C.; Antonopoulus, K.A.; Gioti, F. Numerical simulation of cooling energy consumption in connection with thermostat operation mode and comfort requirements for Athens buildings. *Appl. Energy* **2011**, *88*, 2871–2884. [CrossRef]
17. Sánchez-García, D.; Rubio-Bellido, C.; Martín del Río, J.J.; Pérez-Fargallo, A. Towards the quantification of energy demand and consumption through the adaptive comfort approach in mixed mode office buildings considering climate change. *Energy Build.* **2019**, *187*, 173–185. [CrossRef]
18. Ming, R.; Yu, W.; Zhao, X.; Liu, Y.; Li, B.; Essah, E.; Yao, R. Assessing energy saving potentials of office buildings based on adaptive thermal comfort using a tracking-based method. *Energy Build.* **2020**, *208*, 109611. [CrossRef]

19. Mui, K.W.; Wong, L.T.; Cheung, C.T.; Yu, H.C. Improving cooling energy efficiency in Hong Kong offices using demand-controlled ventilation (DCV) and adaptive comfort temperature (ACT) systems to provide indoor environmental quality (IEQ) acceptance. *HKIE Trans.* **2017**, *24*, 78–87. [CrossRef]

20. Roussac, A.C.; Steinfeld, J.; de Dear, R. A preliminary evaluation of two strategies for raising indoor air temperature setpoints in office buildings. *Archit. Sci. Rev.* **2011**, *54*, 148–156. [CrossRef]

21. Akram Hossain, M.; Khalilnejad, A.; Haddadian, R.; Pickering, E.M.; French, R.H.; Abramson, A.R. Data analytics applied to the electricity consumption of office buildings to reveal building operational characteristics. *Adv. Build. Energy Res.* **2020**. [CrossRef]

22. Franco, A.; Miserocchi, L.; Testi, D. HVAC Energy Saving Strategies for Public Buildings Based on Heat Pumps and Demand Controlled Ventilation. *Energies* **2021**, *14*, 5541. [CrossRef]

23. Traylor, C.; Zhao, W.; Tao, Y.X. Utilizing modulating-temperature setpoints to save energy and maintain alliesthesia-based comfort. *Build. Res. Inf.* **2019**, *47*, 190–201. [CrossRef]

24. Kim, S.K.; Hong, W.H.; Hwang, J.H.; Jung, M.S.; Park, Y.S. Optimal Control Method for HVAC Systems in Offices with a Control Algorithm Based on Thermal Environment. *Buildings* **2020**, *10*, 95. [CrossRef]

25. Jazizadeh, F.; Joshi, V.; Battaglia, F. Adaptive and distributed operation of HVAC systems: Energy and comfort implications of active diffusers as new adaptation capacities. *Build. Environ.* **2020**, *186*, 107089. [CrossRef]

26. Lourenço, J.M.; Aelenei, L.; Facão, J.; Gonçalves, H.; Aelenei, D.; Pina, J.M. The Use of Key Enabling Technologies in the Nearly Zero Energy Buildings Monitoring, Control and Intelligent Management. *Energies* **2021**, *14*, 5524. [CrossRef]

27. Kalaimani, R.; Jain, M.; Keshav, S.; Rosenberg, C. On the interaction between personal comfort systems and centralized HVAC systems in office buildings. *Adv. Build. Energy Res.* **2020**, *14*, 129–157. [CrossRef]

28. Van der Linden, A.A.; Boerstra, A.C.; Raue, A.K.; Kurvers, A.R.; de Dear, R.J. Adaptive temperature limits: A new guidelines in The Netherlands A new approach for the assessment of building performance with respect to thermal indoor climate. *Energy Build.* **2006**, *38*, 8–17. [CrossRef]

29. Rijal, H.B.; Yoshida, K.; Humphreys, M.A.F.; Nicol, J. Development of an adaptive thermal comfort model for energy-saving building design in Japan. *Archit. Sci. Rev.* **2021**, *64*, 109–122. [CrossRef]

30. Hellwin, R.T.; Teli, D.; Schweiker, M.; Choi, J.H.; Lee, M.C.J.; Mora, R.; Rawal, R.; Wang, Z.; Al-Atrash, F. A framework for adopting adaptive thermal comfort principles in design and operation of buildings. *Energy Build.* **2019**, *205*, 109476. [CrossRef]

31. Breesch, H.; Janssens, A. Performance evaluation of passive cooling in office buildings based on uncertainty and sensitivity analysis. *Sol. Energy* **2010**, *84*, 1453–1467. [CrossRef]

32. Psomas, T.; Heiselberg, P.; Lyme, T.; Duer, K. Automated roof window control system to address overheating on renovated houses: Summertime assessment and intercomparison. *Energy Build.* **2017**, *138*, 35–46. [CrossRef]

33. O'Donovan, A.; Murphy, M.D.; O'Sullivan, P.D. Passive control strategies for cooling a non-residential nearly zero energy office: Simulated comfort resilience now and in the future. *Energy Build.* **2021**, *231*, 110607. [CrossRef]

34. Fratean, A.; Dobra, P. Control strategies for decreasing energy costs and increasing self-consumption in nearly zero-energy buildings. *Sustain. Cities Soc.* **2018**, *39*, 459–475. [CrossRef]

35. Gonzalez, R.M.; Torbaghan, S.S.; Gibescu, M.; Cobben, S. Harnessing the flexibility of thermostatic loads in microgrids with solar power generation. *Energies* **2016**, *9*, 547. [CrossRef]

36. Darakdjian, Q.; Billé, S.; Inard, C. Data mining of building performance simulations comprising occupant behaviour modelling. *Adv. Build. Energy Res.* **2019**, *13*, 57–173. [CrossRef]

37. Salom, J.; Widén, J.; Candanedo, J.; Byskov, K. Lindberg, Analysis of grid interaction indicators in net zero-energy buildings with sub-hourly collected data. *Adv. Build. Energy Res.* **2015**, *9*, 89–106. [CrossRef]

38. O'Donovan, A.; O'Sullivan, P.D.; Murphy, M.D. Predicting air temperatures in a naturally ventilated nearly zero energy building: Calibration, validation, analysis and approaches. *Appl. Energy* **2019**, *250*, 991–1010. [CrossRef]

39. Murphy, M.D.; O'Sullivan, P.D.; da Graça, G.C.; O'Donovan, A. Development, Calibration and Validation of an Internal Air Temperature Model for a Naturally Ventilated Nearly Zero Energy Building: Comparison of Model Types and Calibration Methods. *Energies* **2021**, *14*, 871. [CrossRef]

40. Minarčík, P.; Procházka, H.; Gulan, M. Advanced Supervision of Smart Buildings Using a Novel Open-Source Control Platform. *Sensors* **2021**, *21*, 160. [CrossRef]

41. Tumminia, G.; Guarino, F.; Longo, S.; Aloisio, D.; Cellura, S.; Sergi, F.; Brunaccini, G.; Antonucci, V.; Ferraro, M. Grid interaction and environmental impact of a net zero energy building. *Energy Convers. Manag.* **2020**, *203*, 112228. [CrossRef]

42. Aelenei, D.; Lopes, R.A.; Aelenei, L.; Gonçalvesc, H. Investigating the potential for energy flexibility in an office building with a vertical BIPV and PV roof system. *Renew. Energy* **2019**, *137*, 189–197. [CrossRef]

43. Hemanth, G.R.; Raja, S.C.; Nesamalar, J.J.D.; Kumar, J.S. Cost effective energy consumption in a residential building by implementing demand side management in the presence of different classes of power loads. *Adv. Build. Energy Res.* **2020**. [CrossRef]

44. Stasi, R.; Liuzzi, S.; Paterno, S.; Ruggiero, F.; Stefanizzi, P.; Stragapede, A. Combining bioclimatic strategies with efficient HVAC plants to reach nearly-zero energy building goals in Mediterranean climate. *Sustain. Cities Soc.* **2020**, *63*, 102479. [CrossRef]

45. Franco, A.; Fantozzi, F. Experimental analysis of a self-consumption strategy for residential building: The integration of PV system and geothermal heat pump. *Renew. Energy* **2016**, *86*, 1075–1085. [CrossRef]

46.   Tien, P.W.; Wei, S.; Calautit, J. A Computer Vision-Based Occupancy and Equipment Usage Detection Approach for Reducing Building Energy Demand. *Energies* **2021**, *14*, 156. [CrossRef]
47.   Ascione, F.; Bianco, N.; De Masi, R.F.; de Rossi, F.; Vanoli, G.P. Concept, Design and Energy Performance of a Net Zero-Energy Building in Mediterranean Climate. *Proc. Eng.* **2016**, *169*, 26–37. [CrossRef]
48.   Ascione, F.; Borrelli, M.; De Masi, R.F.; de Rossi, F.; Vanoli, G.P. A framework for NZEB design in Mediterranean climate: Design, building and set-up of a lab-small villa. *Sol. Energy* **2019**, *184*, 11–29. [CrossRef]
49.   *UNI EN 15251: 2008 Indoor Environmental Input Parameters for Design and Assessment of Energy Performance of Buildings Addressing Indoor Air Quality, Thermal Environment, Lighting and Acoustics*; UNI: Milan, Italy, 2008.
50.   Carlucci, S.; Bai, L.; de Dear, R.; Yang, L. Review of adaptive thermal comfort models in built environmental regulatory documents. *Build. Environ.* **2018**, *137*, 73–89. [CrossRef]
51.   De Dear, R.J.; Brager, G.S. Developing an adaptive model of thermal comfort and preference. *ASHRAE Trans.* **1998**, *104*, 145–167.
52.   ISSO 74:2014, Termische behaaglijkheid. *Eisen en Achtergronden Betreffende het Thermisch Binnenklimaat in Kantoren, Scholen en Vergelijkbare Utiliteitsbouw*; ISSO: Rotterdam, The Netherlands, 2014. (In Dutch)
53.   *UNI EN 16798-1:2019, Energy Performance of Buildings—Ventilation for Buildings—Part 1: INDOOR Environmental Input Parameters for Design and Assessment of Energy Performance of Buildings Addressing Indoor Air Quality, Thermal Environment, Lighting and Acoustics—Module M1-6*; UNI: Milan, Italy, 2019.
54.   Li, B.; Yao, R.; Wang, Q.; Pan, Y. An introduction to the Chinese Evaluation Standard for the indoor thermal environment. *Energy Build.* **2014**, *82*, 27–36. [CrossRef]
55.   Decree of President of Italian Republic, D.P.R. 412/1993—Requisiti e Dimensionamento Degli Impianti Termici. Available online: https://www.apeapz.it/images/PDF/CaldaiaSicura/Leggi/DPR_412_93.pdf (accessed on 15 June 2021). (In Italian).
56.   *UNI EN ISO 7730:2006, Ergonomics of the Thermal Environment—Analytical Determination and Interpretation of Thermal Comfort Using Calculation of the PMV and PPD Indices and Local Thermal Comfort Criteria*; UNI: Milan, Italy, 2006.
57.   Ascione, F.; Borrelli, M.; De Masi, R.F.; de Rossi, F.; Vanoli, G.P. Hourly operational assessment of HVAC systems in Mediterranean Nearly Zero-Energy Buildings: Experimental evaluation of the potential of ground cooling of ventilation air. *Renew. Energy* **2020**, *155*, 950–968. [CrossRef]
58.   U.S. Department of Energy. *Energy Plus Simulation Software, Version 8.1.0*; U.S. Department of Energy: Washington, DC, USA, 2020.
59.   Design Builder. v. 6.0. 2018. Available online: https://doi.org/10.1016/j.renene.2020.03.180 (accessed on 25 June 2020).
60.   U.S. Department of Energy. Federal Energy Management Program. M&G Guidelines: Measurement and Verification of Performance-Based Contacts Version 4.0. 2015. Available online: https://www.academia.edu/32378615/M_and_V_Guidelines_Measurement_and_Verification_for_Performance_Based_Contracts_Version_4_0 (accessed on 15 June 2021).